UNIVERSIDADE FEDERAL FLUMINENSE
INSTITUTO DE GEOCIÊNCIAS
DEPARTAMENTO DE GEOLOGIA E GEOFÍSICA
PROGRAMA DE PÓS-GRADUAÇÃO EM DINÂMICA DOS OCEANOS E DA TERRA

CARLOS ALBERTO CARDEAL DE JESUS

MULTIATTRIBUTE FRAMEWORK ANALYSIS FOR EVALUATING THE POTENTIAL HIDROCARBON RESERVOIR IN SILICICLASTIC AND CARBONATE ENVIRONMENTS

NITERÓI
2018

CARLOS ALBERTO CARDEAL DE JESUS

MULTI-ATTRIBUTE FRAMEWORK ANALYSIS FOR EVALUATING THE POTENTIAL HIDROCARBON RESERVOIR IN SILICICLASTIC AND CARBONATE ENVIRONMENTS

Dissertation submitted to the Programa de Pós-Graduação em Dinâmica dos Oceanos e da Terra of Universidade Federal Fluminense in partial fulfillment of the requirements for the degree of Master in Geology and Geophysics.

PhD. Wagner Moreira Lupinacci (Principal Adviser)

NITERÓI - RJ
2018

Ficha catalográfica automática - SDC/BIG

D278m De Jesus, Carlos Alberto Cardeal
MULTI-ATTRIBUTE FRAMEWORK ANALYSIS FOR EVALUATING THE POTENTIAL HIDROCARBON RESERVOIR IN SILICICLASTIC AND CARBONATE ENVIRONMENTS / Carlos Alberto Cardeal De Jesus ; Wagner Moreira Lupinacci, orientador. Niterói, 2018.
52 p. : il.

Dissertação (mestrado)-Universidade Federal Fluminense, Niterói, 2018.

DOI: http://dx.doi.org/10.22409/PPGDOT .2018.m.09883808704

1. Decomposição Espectral. 2. Caracterização sísmica. 3. Atríbutos sísmicos. 4. Reservatório carbonático do pré sal. 5. Produção intelectual. I. Título II. Moreira Lupinacci,Wagner , orientador. III. Universidade Federal Fluminense. Instituto de Geociências.

CDD -

Bibliotecária responsável: Yolle Vacariuc Bittencourt - CRB7/6040

MULTI-ATTRIBUTE FRAMEWORK ANALYSIS FOR EVALUATING THE POTENTIAL HIDROCARBON RESERVOIR IN SILICICLASTIC AND CARBONATE ENVIRONMENTS

CARLOS ALBERTO CARDEAL DE JESUS

Dissertation submitted to the Programa de Pós-Graduação em Dinâmica dos Oceanos e da Terra of Universidade Federal Fluminense in partial fulfillment of the requirements for the degree of Master in Geology and Geophysics.

Approved for the Committee in March 06th, 2018.

Committee:

_____

PhD. Djalma Manoel Soares Filho (Petrobras)

_____

PhD. Jobel Lourenço Pinheiro Moreira (Karron)

_____

PhD. Luiz Alberto Santos (Petrobras and UFF)

_____

PhD. Wagner Moreira Lupinacci (GIECAR/GGO/UFF) (Principal Adviser)

Abstract

Petroleum companies have invested heavily in the exploration of new frontier offshore basins in Brazil. Uncertainties associated with geological complexity, lithostratigraphy, fluid content, and seismic resolution in these basins are the most faced challenges. Many methods have been used to circumvent these issues, such as assessing seismic attributes, seismic inversion, spectral decomposition, and the integration of these methodologies to accomplish an optimal approach. Due to the complex geology of these areas, it is very difficult to identify potential reservoirs along one specific geological formation. Hence, applying spectral decomposition to new frontier basins of high geological complexity can help the overcoming of these challenges since, in the frequency domain, it is possible to better define variability and lateral geologic discontinuities. However, without the support of other geophysical methods, this approach may increase rather than reduce uncertainties. The correct choice of the spectral decomposition optimization approach is crucial to guarantee that the target zone is accurately represented and is as crucial as selecting the appropriate transform. Here, with the objective to reduce risk in exploration and development phase, we present two methodologies which integrates different types of seismic attributes as well as elastic inversion, spectral decomposition and geometrical attributes and seismic facies classification in Brazilian siliciclastic and carbonate environment. First methodology applied in Brazilian equatorial margin basin, the result shows the new appraisal well had been planned at a good location, but that its facies were not as good as those of the first discovery well (fact confirmed after drilling). The second methodology applied in brazilian pre sal carbonate, shows that the multi-attribute analysis and facies classification to generate a geologically significant outcome and to guide a final geobody extraction that is calibrated by well data and that can be used as a spatial indicator of the distribution of good reservoir quality for static modeling.

Keywords: spectral decomposition, new frontier basins, seismic facies, Brazilian equatorial margin basin.

Resumo

As empresas de petróleo têm investido fortemente na exploração de bacias *offshore* de novas fronteiras no Brasil. Incertezas associadas à complexidade geológica, litoestratigrafia, presença de fluidos e resolução sísmica nessas bacias são os desafios mais enfrentados. Muitos métodos têm sido utilizados para contornar essas questões, tais como a avaliação de atributos sísmicos, inversão sísmica, decomposição espectral e a integração dessas metodologias para obter uma melhor abordagem. Devido à complexa geologia dessas áreas, é muito difícil identificar potenciais reservatórios de hidrocarbonatos ao longo de uma formação geológica específica. Assim, a aplicação da decomposição espectral as bacias de novas fronteiras de alta complexidade geológica podem auxiliar na superação desses desafios, pois no domínio da frequência, é possível melhor definir variabilidade e descontinuidades geológicas laterais. No entanto, sem o apoio de outros métodos geofísicos, esta abordagem pode aumentar as incertezas em vez de reduzí-las. Por isso, a escolha correta da abordagem de otimização da decomposição espectral é crucial para garantir que a zona alvo seja representada com precisão e é tão crucial quanto escolher a transformada apropriada para decompor o dado sísmico. Aqui, com o objetivo de reduzir o risco na fase de exploração e desenvolvimento, apresentamos duas metodologias que integra diferentes tipos de atributos sísmicos, como os atributos resultantes da inversão elástica e da decomposição espectral e atributos geométricos e a classificação de fáceis sísmicas em ambientes siliciclásticos e carbonáticos do pré-sal brasileiro. Na primeira metodologia, aplicada numa bacia da margem equatorial brasileira, os resultados mostraram que o novo poço de avaliação foi planejado em uma boa localização, mas que suas fácies não eram tão boas quanto as do primeiro poço descoberto (fato confirmado após a perfuração). Na segunda metodologia, aplicada nos carbonatos do pré-sal brasileiro, a análise multi-attributo e a classificação de fácies sísmica contribuíram para gerar um resultado geologicamente significativo e guiar uma extração de um *geobody*, calibrada por dados de poços e que pode ser usada como um indicador espacial da distribuição de boa qualidade de reservatório para modelagem estática.

Palavras-chave: Decomposição espectral, bacias de novas fronteiras, sismofácies, bacias de margem equatorial brasileira.

Acknowledgements

First, I would like to thank God and to express my very profound gratitude to my family for providing me with unconditional support and continuous encouragement throughout my years of study and through the process of researching and writing this thesis. This accomplishment would not have been possible without them.

I would also like to thank my thesis advisor Wagner Lupinacci. He was always willing to help whenever I ran into a trouble spot or had a question about my research or writing. He consistently allowed this paper to be my own work but steered me in the right direction whenever he thought I needed it.

I would also like to thank the experts who were involved in the validation survey for this research project: the geologists Maria Olho Azul and Patrícia Takayama. Without their passionate participation and input, the validation survey could not have been successfully conducted

Thanks, ANP institution, for making the necessary data available for the accomplishment of this work.

Finally, I would like to thank this great university (Universidade Federal Fluminense) for always being part of the great victories in my life.

"I will instruct you and teach you the way you should go; I will counsel and take care of you. "Psalm 8:32.

Contents

Abstract i

Resumo ii

1. Presentation 4

1.1. Dissertation structure 4

2. Introduction: Siliciclastic Environment 5

3. Methodology: Article 1 7

3.3. Pre-stack inversion 12

3.4. Spectral decomposition 12

3.5. Seismic facies classification 15

4. Results and Discussions: Article 1 17

5. Introduction: Carbonate Environment 25

6. Methodology: Article 2 28

6.1. Seismic data acquisition and processing overview 29

6.2. Preconditioning of seismic data 30

6.3. Calculation of seismic attributes 31

6.4. Seismic facies classification 38

7. Results and Discussions: Article 2 42

8. Conclusions 44

8.1. Conclusions of the Article 1 44

8.2. Conclusion of the Article 2 44

References 45

List of Figures

Figure 1: Submarine canyons showing the complex bathymetry of the study area, which impact the seismic imaging of the reservoir zone. 8

Figure 2: Seismic processing workflow applied for improved seismic imaging. 9

Figure 3: (a) Original seismic section. (b) Seismic section after application of the structurally-oriented filtering. (c) Seismic section after application of the spectral enhancement. It is possible to notice the increase of the seismic resolution after preconditioning and better definition of layers as shown in the red boxes. 10

Figure 4: (a) Maximum negative amplitude and; (b) Dominant frequency (Hz) extracted between the top and base of the reservoir. The wells are represented by stars. 13

Figure 5: Short-time Window Fourier Transform (SWFT) applied to seismic data, decomposing it into frequency bands, and then envelope attributes were calculated for each frequency band. 14

Figure 6: Envelope attributes: (a) red for low frequency (10 Hz), (b) green for mid frequency (20 Hz) and, (c) blue for high frequency (30 Hz), showing how the RGB blend (d) was created. 15

Figure 7: Section view of an arbitrary line crossing discovery and appraisal wells of (a) acoustic impedance values and (b) Vp/Vs ratio values. 18

Figure 8: (a) Cross plot between the acoustic impedance and Vp/Vs ratio discovery well logs colored by the clay volume log with polygons highlighting the good-quality sandstones and shales, (b) section view of an arbitrary line in the seismic impedance volume which the good-quality sandstones are highlighted according to the cross plot and (c) section view of an arbitrary line in the seismic impedance volume which the shales are highlighted according to the cross plot. 19

Figure 9: Sections with: (a) probabilities of good-quality sandstones, (b) probabilities of shales, (c) probabilities of poor-quality sandstones and (d) most probable facies compared with the facies log from the discovery well. Two-way traveltime (TWT). 20

Figure 10: Quality control comparison of spectral decomposition RGB blends in the depth (a) and time (b) domains from a horizon slice. 21

Figure 11: Enhanced view of the spectral decomposition RGB blend for (a) both the discovery and appraisal wells in the study area, (b) zooming in the discovery well (c) zooming in appraisal well. 22

Figure 12: Section view of an arbitrary line crossing the discovery and appraisal wells of seismic facies classification results. 23

Figure 13: Gamma ray and total porosity logs versus seismic facies classification at the discovery well (a) and at the appraisal well (b) locations. 23

Figure 14: Steps used to calculate the seismic attributes..... 28

Figure 15: Preconditioning. (a) Input; (b) SOF; (c) Imaging enhancement. 31

Figure 16: Curvature attribute in two dimensions, indicating that this attribute is positive in an anticline, negative in a syncline, and zero in a flat or dipping plane. 32

Figure 17: Spatial (or multitrace) analysis windows used to calculate the coherence attribute (W is defined as the vertical analysis window for time T)..... 33

Figure 18: Dominant frequency. (a) Root mean square amplitude; (b) maps. 34

Figure 19: Schematic of stage 2 for optimization and application of HSD (Hybrid Spectral Decomposition). First, the STFT (Short Time Fourier Transform) is applied and a frequency band is selected. Then the envelope attribute is calculated. 35

Figure 20: Spectral Decomposition (a), Hybrid Spectral Decomposition (b). 37

Figure 21: The hybrid spectral decomposition pseudo log (black) and the porosity log (red) are well correlated (inversely). These logs were used as a quality control. 37

Figure 22: Curvature (a) and coherence (b) attributes applied to the structural map of the top of the reservoir, revealing faults and fracture zones around the wells. 38

Figure 23: Seismic facies. Structural map of the top of the reservoir, highlighting the carbonate mounds. 40

Figure 24: Illustration of our “360º approach” applied in this work. 41

Figure 25: Geobody of carbonate mounds extracted from seismic facies classification. 43

List of Tables

Table 1: Acquisition parameters. 7

Table 2: Acquisition parameters from a single vessel. 29

Table 3: Correlation between envelope and acoustic impedance. 35

1. Presentation

This dissertation was developed based on the results from two works: Risk evaluate on new frontier basin of brazilian equatorial margin and characterization of brazilian pre-salt carbonate reservoir. In order to develop these two works, I used two different methodologies of combining seismic attributes as well as spectral decomposition, seismic inversion, geometrical attributes and seismic facies classification. These dissertation is presented in the form of two scientific articles, which will be submitted to recognized journals: **THE AMERICAN ASSOCIATION OF PETROLEUM GEOLOGISTS JOURNAL (AAPG)**, with title: **An Approach to Reduce Exploration Risk using Spectral Decomposition, Pre-stack Inversion and Seismic Facies Classification** and **THE SOCIETY OF EXPLORATION GEOPHYSICIST JOURNAL INTERPRETATION (Interpretation),** with title: **MultiAttribute Framework Analysis for the Identification of Carbonate Mounds in The Brazilian Presalt Zone** after all reviews requested by the evaluators are met.

1.1. Dissertation structure

The stages carried out for the development of the dissertation were organized in a total of eight chapters, being: presentation and conclusion, first and the last chapter respectively, will be unique for both articles and introduction, methodology, results and discussions separately for each one.

The second chapter presents the main challanges that motivated the proposed work. In the third chapter is addressed the application of the methodology in the seismic data of brazilian equatorial margin basin with siliciclastic reservoir.

The fourth chapter discusses the results and discussions for the first article. In the fifth chapter we present the introduction of the second article, which will show the challenges faced and the proposals to solve them.

In the sixth chapter is presented the methodology applied in the environments of carbonate reservoirs of the Brazilian pre-salt, followed by the seventh chapter that contains the results and discussions. Finally, the last chapter presents the conclusions obtained through the critical analysis of the results of both articles.

2. Introduction: Siliciclastic Environment

Spectral decomposition transforms temporal signals into energy density maps. There are many methods available to express the energy of the signal as a function of frequency and amplitude. Each method has its advantages and disadvantages, and different applications require different transforms and specific optimization (Castagna and Sun, 2006). Spectral decomposition has been successfully applied in seismic exploration for stratigraphic mapping (Partyka et al., 1999; Marfurt and Kirlin, 2001; Puryear and Castagna, 2008), reservoir detection (Castagna et al., 2003; Sinha et al., 2005) and attenuation estimation and correction (Lupinacci and Oliveira, 2015), therefore helping to decrease uncertainties encountered during the exploration and production phases and assisting the identification of the best regions for drilling new wells (Jesus et al., 2019).

In order to define the best spectral decomposition approach to be used, the application, quality of seismic illumination, frequency range, signal-to-noise ratio and geologic complexity must be taken into account. A good practice is to conduct a feasibility study to establish the most appropriate spectral decomposition method depending of the purpose of its use. In addition, horizon mapping of an extensive seismic survey may result in many errors due to auto-picking, with complex geology limiting the use of horizon slices for spectral decomposition optimization because they cannot represent a geologic timeline. Integration of different seismic attributes, such as compressional (P)- and shear (S)-impedances, compressional velocity and shear velocity (Vp/Vs) ratio, can help overcome these problems.

Pre-stack seismic inversion has been applied as a tool for the quantitative seismic interpretation, helping to characterize reservoirs (see, for example, Avseth et al., 2005; Zhao et al., 2017). The elastic parameters (P- and S-impedances, and Vp/Vs ratio) obtained from seismic inversion are correlated with rock physical models, providing information about lithology, fluid content, and porosity (Spikes et al., 2007; Simm and Bacon, 2014). From the seismic inversion and rock physics modelling, static models of reservoir properties are built and thus can assist in reserves estimation (Vernik et al., 2002), location of production and injection wells and can be used as input for flow simulations in dynamic models (Bredesen et al., 2015; Ferreira and Lupinacci, 2018).

Dominant frequency and maximum negative amplitude are other useful seismic attributes that can contribute to optimization of spectral decomposition. When aiming to analyze the dominant frequency in a target zone interval, it is very important to establish which frequencies best represent the potential reservoir. In addition, the maximum negative amplitude between the top and base of the reservoir should be analyzed to assist in the determination of best areas for production because its response is mostly connected to hydrocarbon anomalies or good quality reservoirs (Jesus et al., 2019).

Finally, seismic facies classification through unsupervised neural network methods is a very powerful tool for reservoir characterization because it allows fast data analysis through the identification of linear or non-linear correlations amongst the input seismic attribute volumes and generates facies expected for the area helping to identify the best reservoir facies when associated to well information (Deboeck and Kohonen, 1998; Du and Swamy, 2014; Shanmuganathan, 2016; Ferreira et al., 2019).

3. Methodology: Article 1

3.1. Seismic data acquisition and processing

The acquisition parameters are shown in Table 1. A 6 km (~3.73 mi) streamer length in an environment with huge submarine canyons and cliffs with bathymetric variation of up to 400 m (~1312.3 ft) (Figure 1). Such an acquisition survey might compromise the rays, resulting in target zone poor illumination. Poor illumination was also observed at the greatest depths because of natural energy absorption and a low contribution from the far offset data due to the short cable length.

Table 1: Acquisition parameters.

Acquisiton parameters	
Minimum offset	137 m (~449.4 ft)
Source separation	37.5 m (~123 ft)
Source interval	12.5 m (~41.0 ft)
Source depth	6.5 m (~21.3 ft)
Number of streamers	8
Streamers separation	75 m (~246.1 ft)
Streamers depth	8 m (~26.2 ft)
Streamers length	6 Km (~3.73 mi)
Group interval	12.5 m (~41.0 ft)
Number of channels	3840
Recording length	9.216 ms
Sampling rate	2 ms

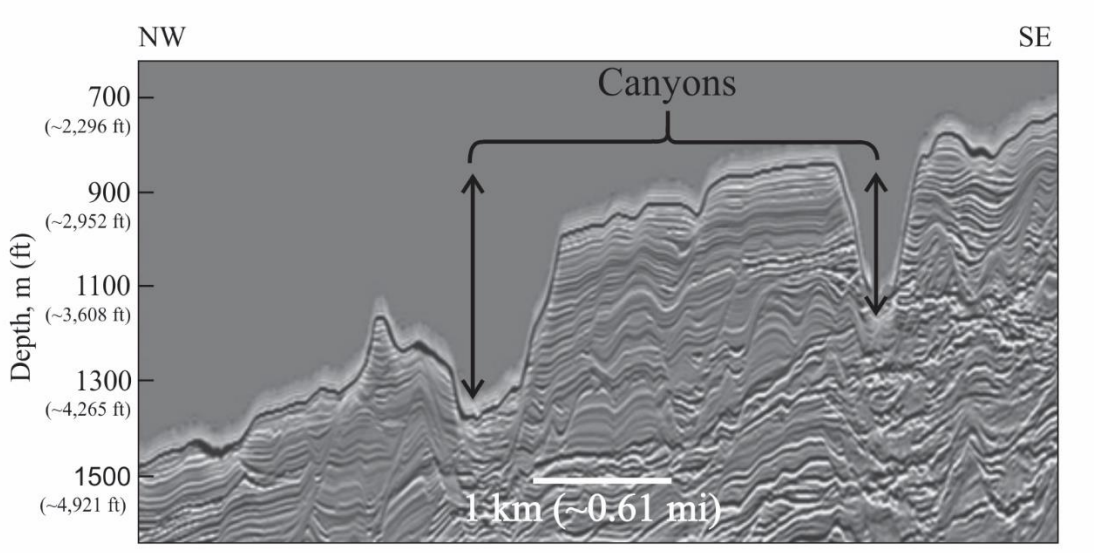

Figure 1: Submarine canyons showing the complex bathymetry of the study area, which impact the seismic imaging of the reservoir zone.

In order to obtain better images from the subsurface, the seismic data was processed using a specific workflow. The complete flowchart is presented in Figure 2. The complete seismic processing history is not described here. However, two main steps that were used to achieve considerable analytical improvements are highlighted: water column statics (WCS) correction and velocity model building (VMB). The WCS correction was applied to compensate for velocity changes in the water column caused by salinity, temperature and density. As for VBM, the initial step applied was a tomographic model. Then, a tilted transversal isotropic (TTI) model was obtained from the tomographic approach, along with three seismic and well data inversions (Bakulin et al., 2010). In order to decrease the well-to-seismic misties, the anisotropy models were updated based on well markers.

An important strategy was adopted in the data processing to prevent the velocity model from following seafloor variation or creating “bull eyes” in the final model, which consisted of building the velocity model starting with the low frequencies and to refining it by adding the higher frequencies in each round of tomography. Occasionally, the tomographic signal was lost, converging to a local minimum due to poor illumination associated with the highly complex seafloor topography.

The initial step of VMB, we applied a tomographic model. Then, a tilted transversal isotropic (TTI) model was obtained from the tomographic approach, along

with three seismic and well data inversions (Bakulin et al., 2010). In order to decrease the well-to-seismic mistie, we updated the anisotropy models based on the well markers.

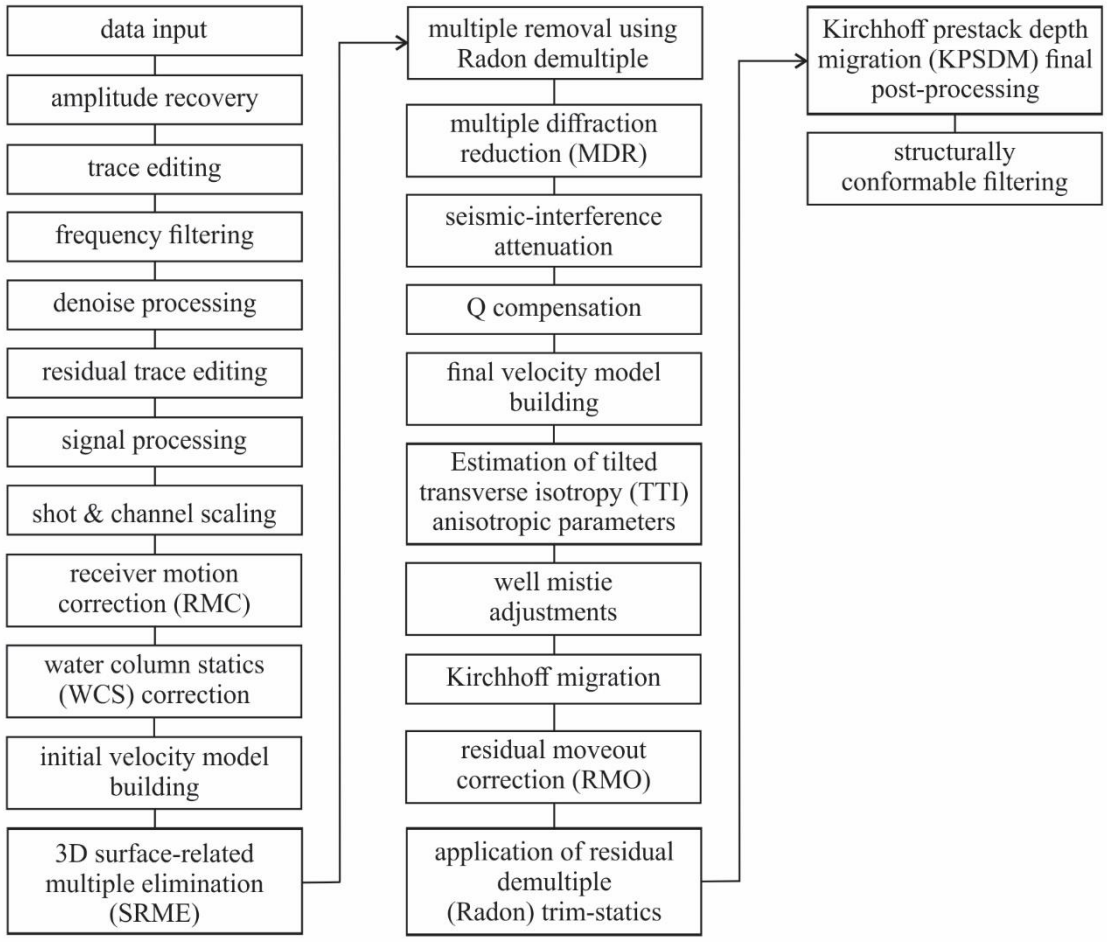

Figure 2: Seismic processing workflow applied for improved seismic imaging.

Seismic data usually contain random and coherent noise. This noise may be due to acquisition design, preprocessing, and migration (Chopra and Marfurt, 2007). Nevertheless, some of those problems can be mitigated through post-stack processing before generating seismic attributes.

The seismic migration data was preconditioned through two stages, each having different objectives. First, a structurally-oriented filtering was applied to improve the signal/noise ratio, which can make the seismic reflector more continuous, and better define faults. Then, spectral enhancement was used to improve vertical resolution (Zhou et al., 2014). As shown in Figure 3, these steps preserved the original dominant frequency and accentuated the pre-existing frequencies, thereby increasing bandwidth and improving the vertical resolution.

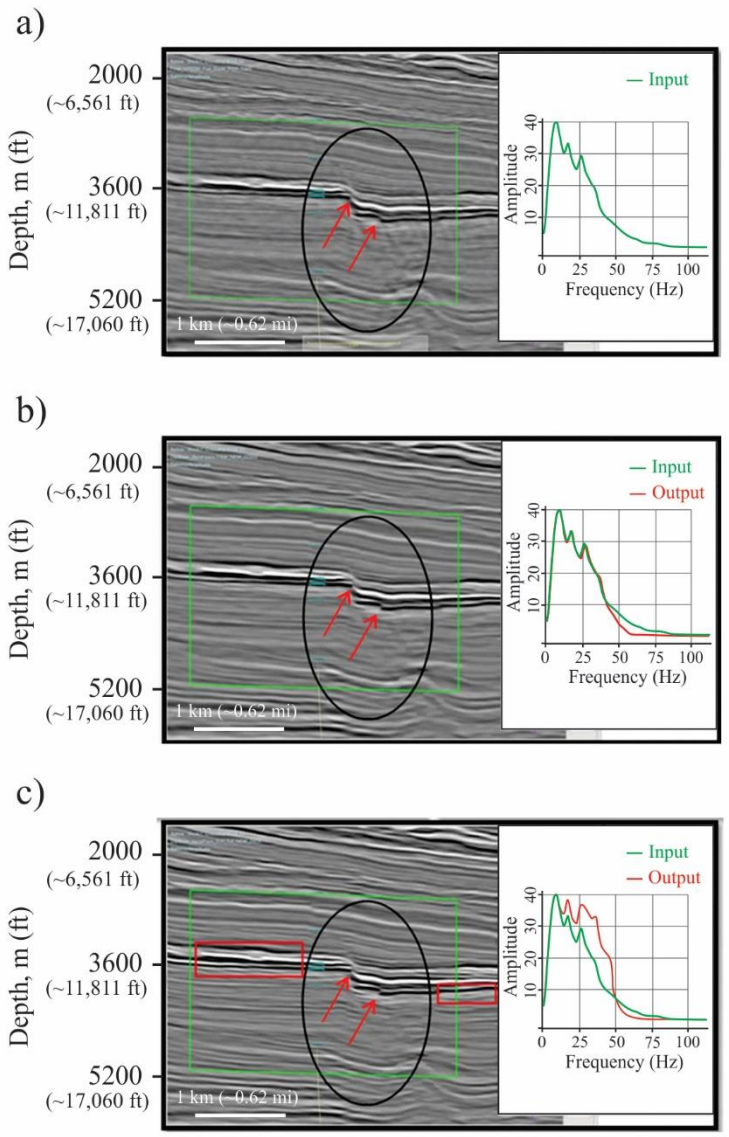

Figure 3: (a) Original seismic section. (b) Seismic section after application of the structurally-oriented filtering. (c) Seismic section after application of the spectral enhancement. It is possible to notice the increase of the seismic resolution after preconditioning and better definition of layers as shown in the red boxes.

3.2. Seismic data preconditioning

Seismic data usually contain random and coherent noise. This noise may be due to acquisition design, preprocessing, and migration (Chopra and Marfurt, 2007). Nevertheless, some of those problems can be mitigated through post-stack processing before generating seismic attributes.

The seismic migration data was preconditioned through two stages, each one having different objectives. We first applied structurally-oriented filtering to improve the signal/noise ratio, which can make the seismic reflector more continuous, and better

define faults. Then, we applied spectral enhancement to improve vertical resolution (Zhou et al., 2014). As shown in Figure 3, these steps preserved the original dominant frequency and accentuated the pre-existing frequencies, thereby increasing bandwidth and improving the vertical resolution.

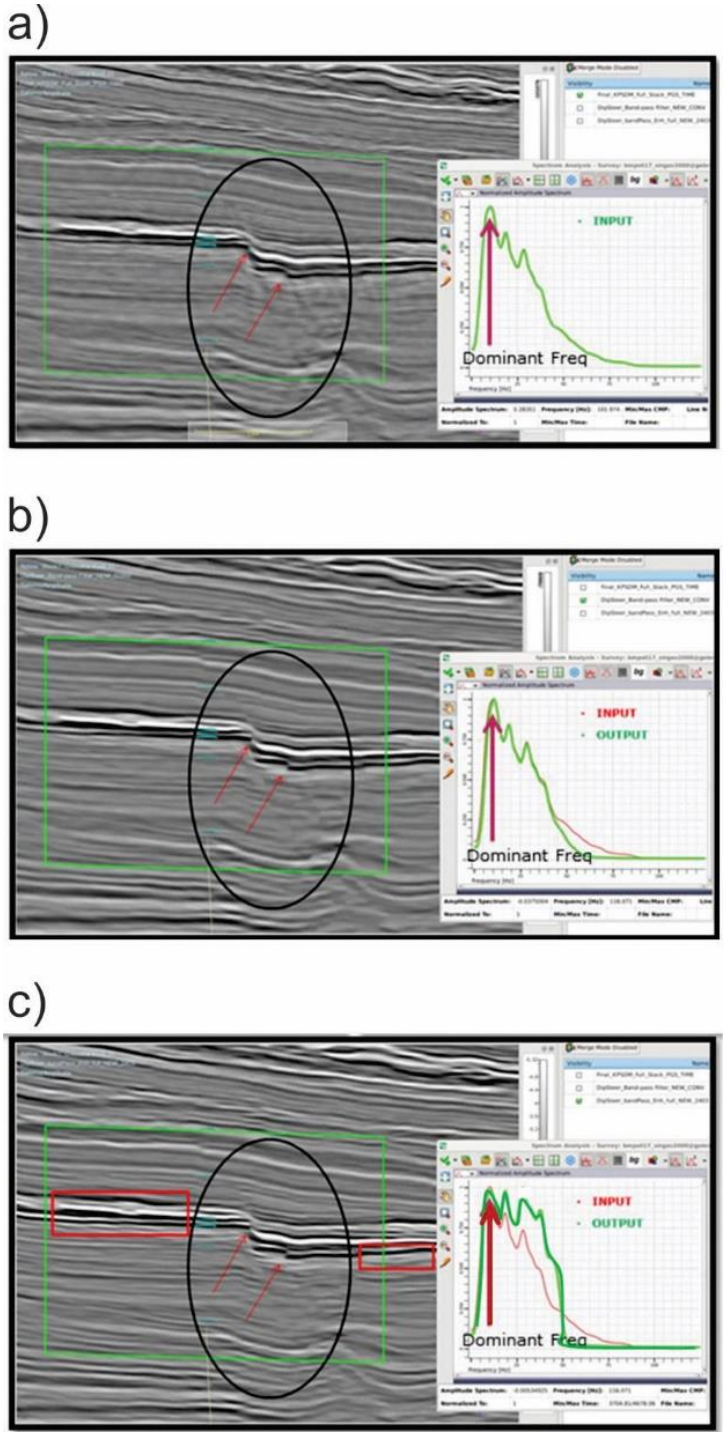

Figure 3: (a) Original seismic data used as input. (b) Result of structurally-oriented filtering. (c) Spectral enhancement.

3.3. Pre-stack inversion

Information obtained from pre-stack inversion may facilitate the identification of facies within the target zone. The use of elastic attributes to optimize spectral decomposition can increase the reliability for identification of lithology and fluid type (Jesus and Takayama, 2016). In this study, pre-stack inversion was used to discriminate sands from shales, and spectral decomposition was performed only considering the dominant frequency value corresponding to the sand zones.

When elastic attributes, such as compressional (Vp) and shear (Vs) velocities, acoustic impedance (Ip) and density are known, predictions of petrophysical parameters, characterization of rock heterogeneity and complexity, as well as their uncertainty associated with theoretical modeling, are the main objectives of rock physics inversion (Grana and Della Rossa, 2010). A combination of rock physics inversion and seismic inversion facilitates estimation of petrophysical properties (Grana, 2016) and, when petrophysical properties and their uncertainties can be estimated, it is possible to assess the probable facies occurrence (Xu et al., 2016).

Seismic inversion attributes (Ip and Vp/Vs) and lithological information from the wells were used to obtain facies and fluid probabilities (FFP) through Bayesian inference (Pendrel et al., 2017; Schwedersky et al., 2017). The FFP helped in the uncertainty analysis for reservoir evaluation. Three volumes resulting from FFP analysis based on the construction of probability density functions (PDF) on an Ip and Vp/Vs crossplot were generated: good-quality sandstone reservoir, poor-quality sandstone reservoir, shale, and some unidentified facies.

3.4. Spectral decomposition

Conventional spectral decomposition methodologies consider horizon slices or time slices to optimize their results. However, geologic complexity inhibits the accuracy of these conventional approaches. Focusing solely on the reservoir area, elastic inversion attributes were used to optimize spectral decomposition and to increase the reliability of results, assisting in the interpretations (Veeken and Da Silva, 2004). Then, a sensitivity study was performed using the top and the base of the interpreted horizons from the elastic inversion result, as well as the seismic volume following structurally-oriented filtering and spectral enhancement, to calculate the maximum negative amplitude and dominant

frequency. With the maximum negative amplitude and dominant frequency attributes (Figure 4), both the discovery well and the first appraisal well locations were evaluated. Based on the maximum negative amplitude map, both wells are in a strong negative amplitude zone, but the signal is weaker for the appraisal well.

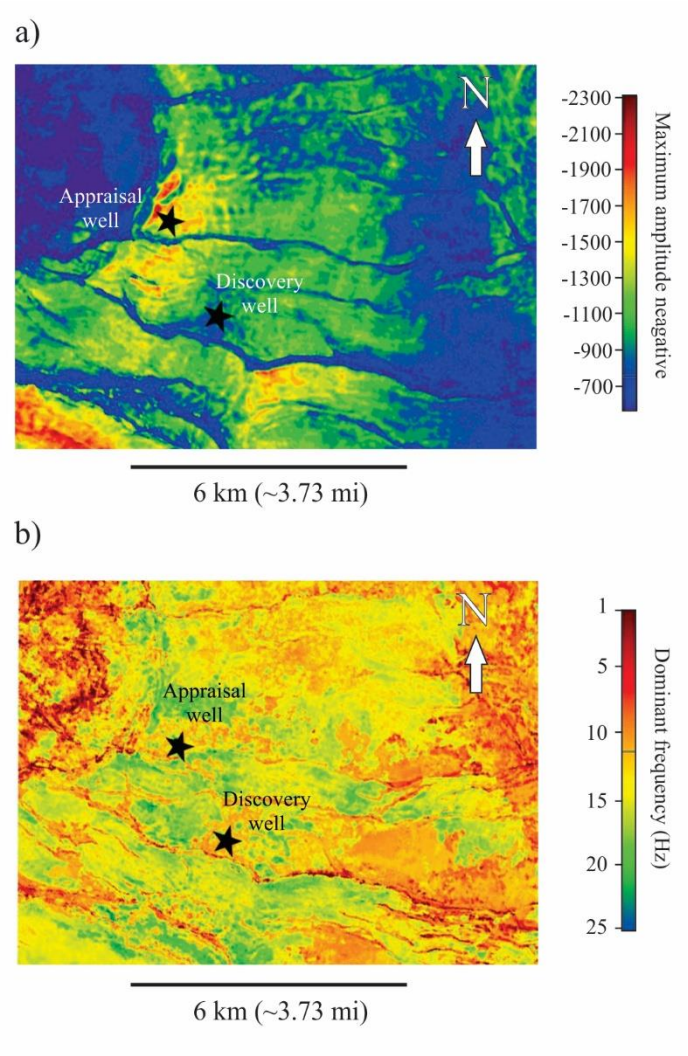

Figure 4: (a) Maximum negative amplitude and; (b) Dominant frequency (Hz) extracted between the top and base of the reservoir. The wells are represented by stars.

Spectral decomposition basically decomposes the seismic data into different frequency bands, as illustrated in Figure 5. The seismic data in the time domain was used for spectral decomposition as the algorithm assesses spectral components in the time-frequency domain (measured in cycles/s or Hz). However, the results are later converted to the depth domain using the existing VMB for enhanced accuracy and to have more control over tuning effects.

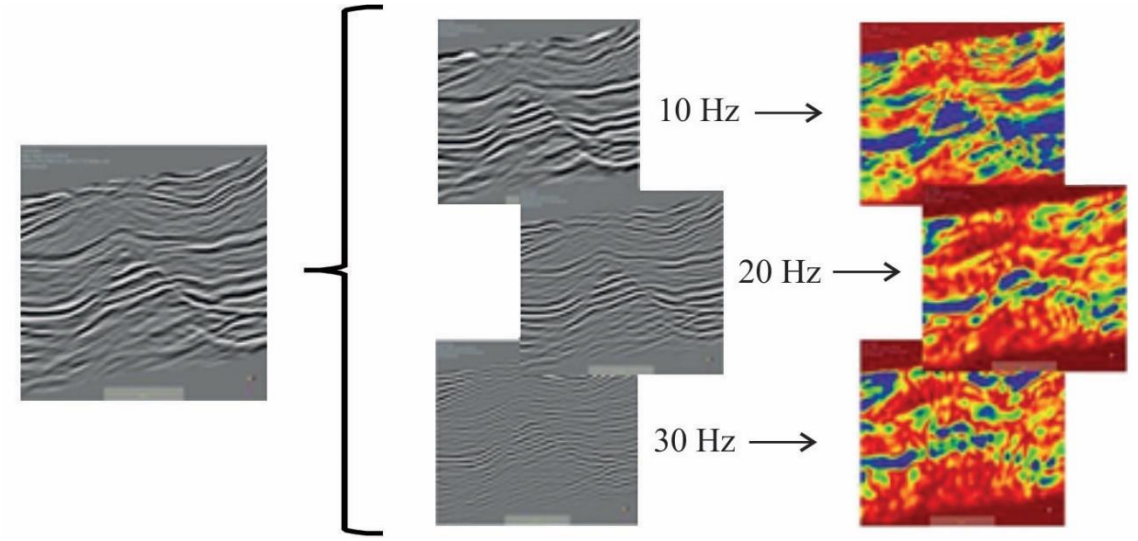

Figure 5: Short-time Window Fourier Transform (SWFT) applied to seismic data, decomposing it into frequency bands, and then envelope attributes were calculated for each frequency band.

Based on the analysis of dominant frequency, the reservoir exhibits mainly a low frequency of 10 Hz. Also, the base of the reservoir has a strong negative amplitude and most important frequencies in the reservoir were identified through a sensitivity study that indicated frequency bands of 10 Hz, 20 Hz and 30 Hz which were used for analysis. Then, the envelope attribute for each of selected frequency bands was calculated (Figure 6) and contained amplitude information for each specific range.

Spectral decomposition using short time window Fourier transform (SWFT) was applied to the seismic volume following preconditioning and spectral enhancement. SWFT spectral decomposition uses a time window, which influences the frequency, as well as temporal and spatial resolutions. Narrower windows provide good vertical resolution but generate low frequency resolution (Addison, 2002). The main objective of using SWFT is to obtain high frequency resolution to better understand the spatial distribution of seismic facies, while balancing this with an acceptable vertical resolution. Therefore, SWFT was applied with a time window of 30ms based on seismic data from well logs and markers. According to Chopra and Marfurt (2014), the window width should be carefully chosen because analysis of windows that are smaller than the period of interest can create Gibbs artifacts.

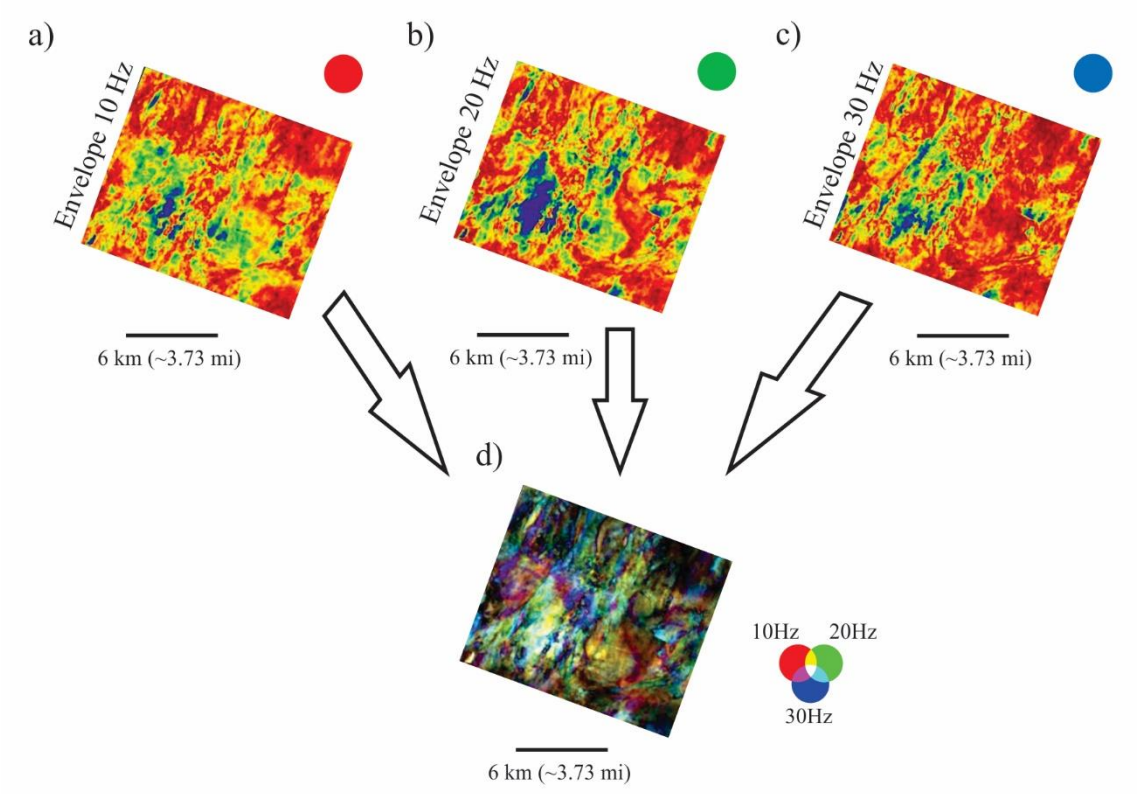

Figure 6: Envelope attributes: (a) red for low frequency (10 Hz), (b) green for mid frequency (20 Hz) and, (c) blue for high frequency (30 Hz), showing how the RGB blend (d) was created.

3.5. Seismic facies classification

An unsupervised neural network was used for seismic facies classification based on self-organizing maps method defined by Kohonen (1990; 2013). The application of this method is based entirely on the characteristics of seismic data and the resulting facies are indicative of reservoir heterogeneity (Jesus et al., 2019).

The combination of different seismic attributes increases analytical complexity for seismic facies classification. Principal Component Analysis (PCA) can be used to assess a large set of seismic attributes (Chopra and Marfurt, 2014) and also helps to reveal the most significant seismic attributes (Roden et al., 2015), thereby minimizing redundancy. To perform a PCA, the spectral decomposition, coherence, acoustic impedance and dominant frequency attributes were selected in order to reveal distribution patterns in the reservoir. Coherence is a measure of similarity between waveforms or traces (Chopra and Marfurt, 2007). This geometrical attribute is helpful to identify faults and fractures, which are important features at the margins of a basin. In addition, acoustic impedance can be an excellent tool to estimate the petrophysical parameters of a reservoir

(Sancevero et al., 2006) and low-frequency seismic anomalies may be associated with reservoirs (Castagna et al., 2003). The first three resulting principal component vectors were used as input for seismic facies classification. As for the unsupervised neural network parametrization, five was the number of classes selected for data discrimination in 60 iterations.

4. Results and Discussions: Article 1

The acoustic impedance and Vp/Vs ratio obtained from pre-stack inversion are shown in Figure **7**a and 7b, respectively. Using the acoustic impedance, Vp/Vs ratio and clay volume discovery well logs crossplot (Figure 8a) it was possible to identify the sandstones that may contain oil (termed "good-quality sandstones") identifiable by intermediate acoustic impedance and low Vp/Vs ratio values. Shales were characterized by low acoustic impedance and high Vp/Vs ratio values. The sandstones with lower probability of oil (termed "poor-quality sandstones") were classified as the rest of the points in the crossplot with high acoustic impedance values and intermediate Vp/Vs ratio values. The regions of good-quality sandstones and shales, using the limits established by the crossplot analysis, in the acoustic impedance volume are highlighted in Figure 8b and 8c, respectively. As can be seen in Figure 8b, both wells are good-quality sandstone locations. The seismic inversion attributes aided in top and bottom mapping and also in optimizing the spectral decomposition and limiting propagation of uncertainty in subsequent steps.

Figure 9a, 9b and 9c show probabilities of each facies in a section and Figure 9d shows the most probable facies, revealing three different facies identified as shales (brown color) at the top of the section, immediately below the good-quality sandstones (green color), and the poor-quality sandstones (yellow color) at the bottom of the section. It is important to highlight that the actual facies of the discovery well show good correlation with the estimated facies.

As for the spectral decomposition results, envelope attributes were calculated for each one of the selected frequencies and created an RGB blend: red for low frequency (10Hz), green for intermediate frequency (20Hz), and blue for high frequency (30Hz). The spectral decomposition RGB blend were compared in time and depth domains as a quality control to verify if both results were consistent (Figure 10).

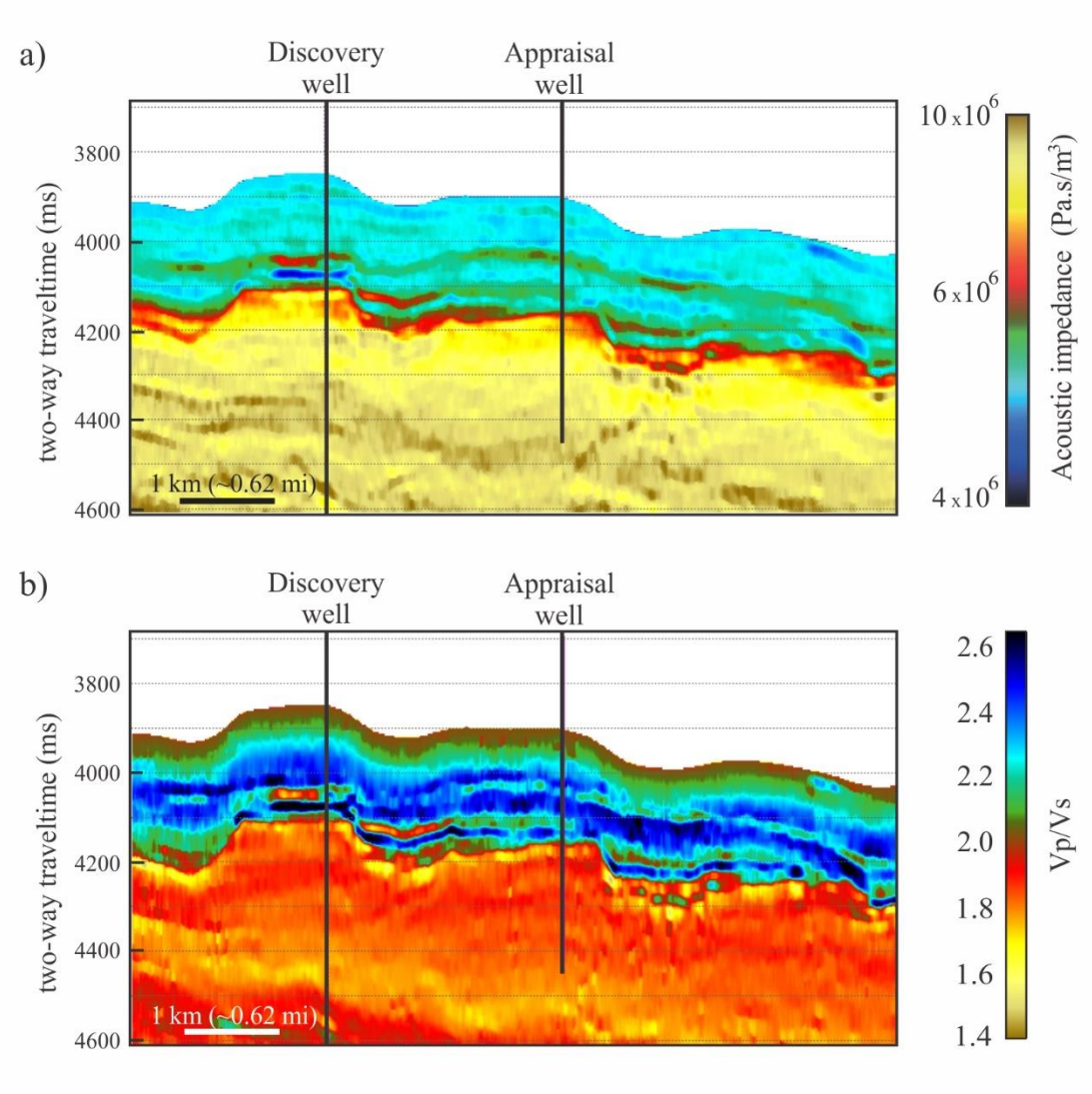

Figure 7: Section view of an arbitrary line crossing discovery and appraisal wells of (a) acoustic impedance values and (b) Vp/Vs ratio values.

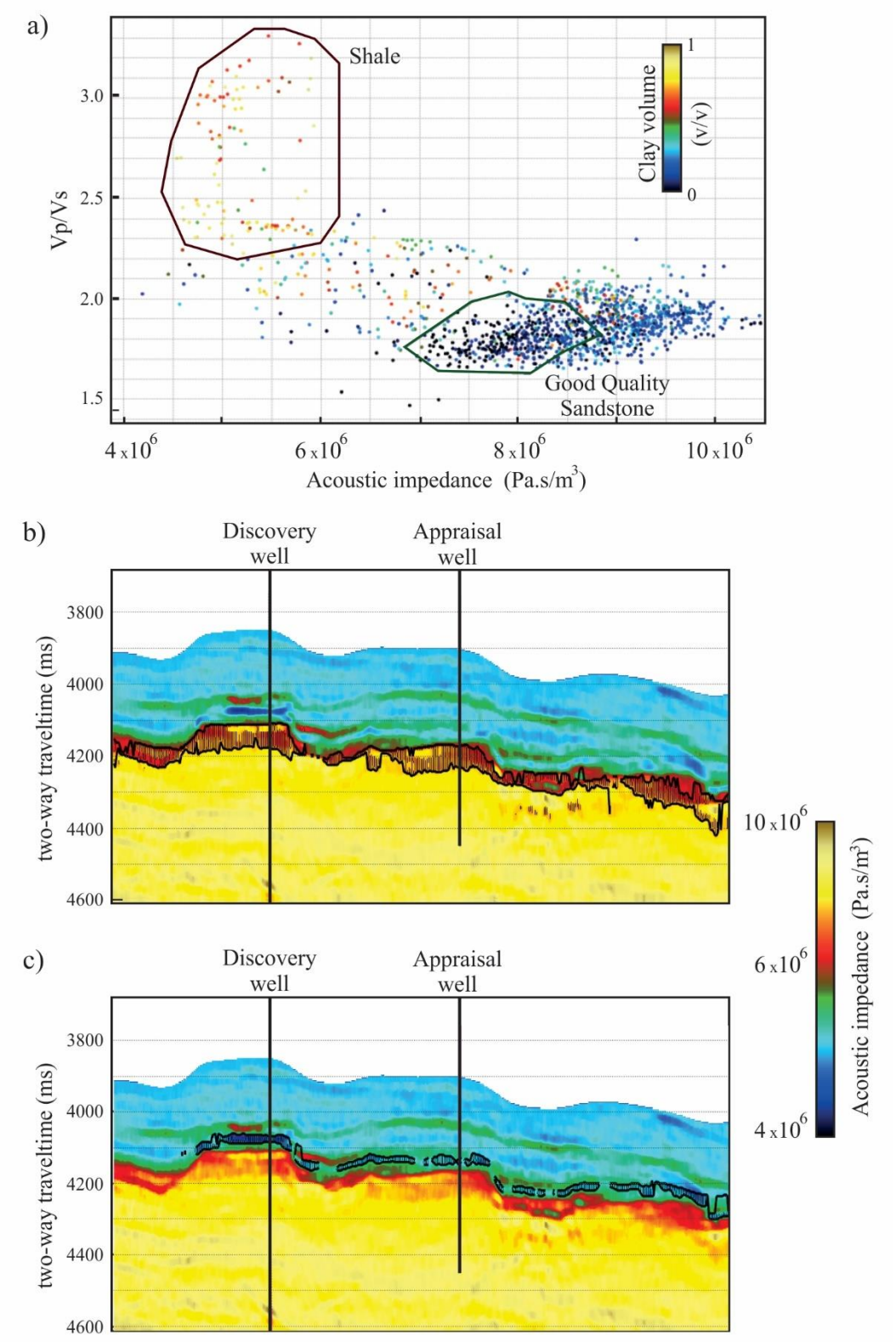

Figure 8: (a) Cross plot between the acoustic impedance and Vp/Vs ratio discovery well logs colored by the clay volume log with polygons highlighting the good-quality sandstones and shales, (b) section view of an arbitrary line in the seismic impedance volume which the good-quality sandstones are highlighted according to the cross plot and (c) section view of an arbitrary line in the seismic impedance volume which the shales are highlighted according to the cross plot.

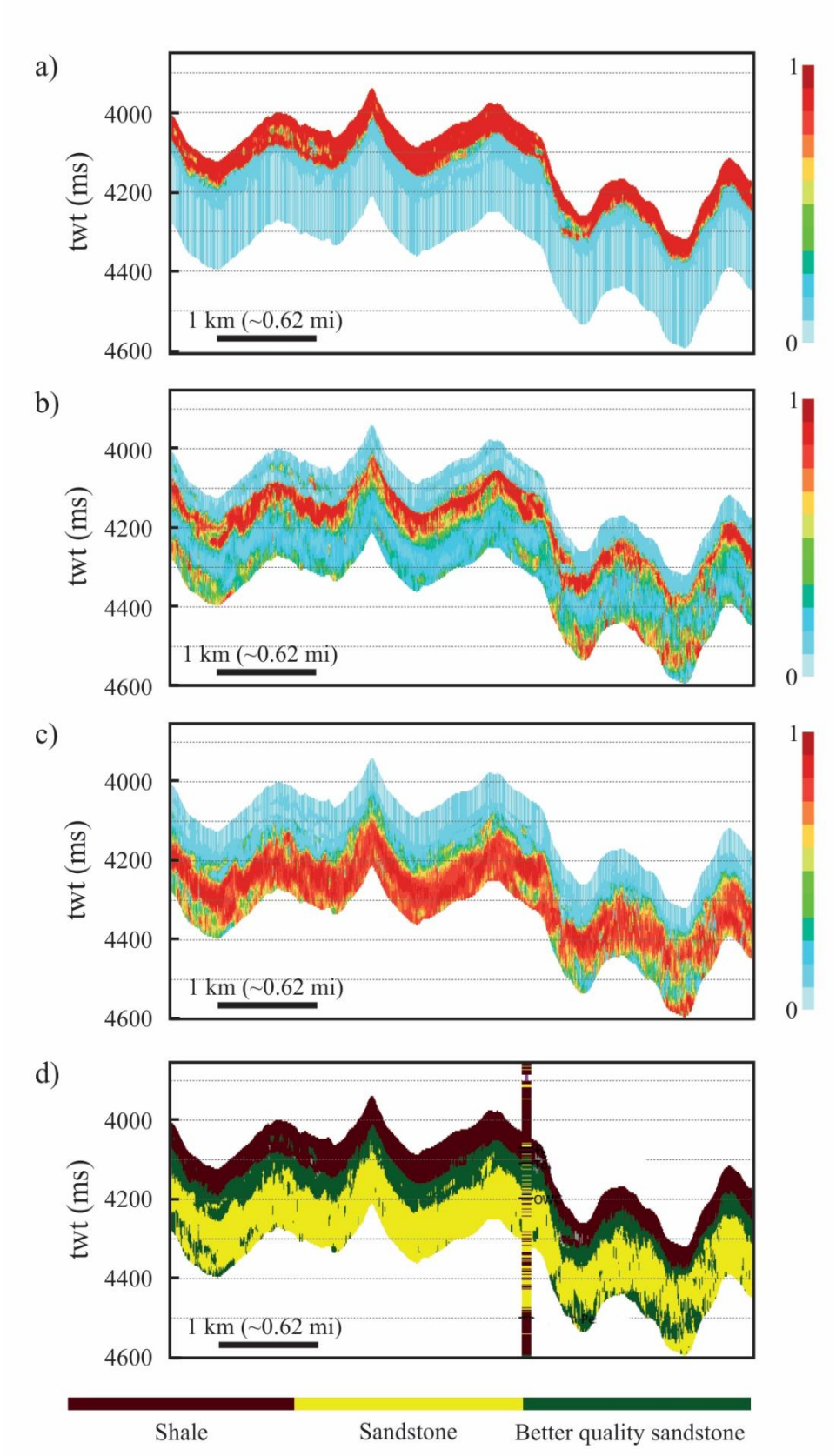

Figure 9: Sections with: (a) probabilities of good-quality sandstones, (b) probabilities of shales, (c) probabilities of poor-quality sandstones and (d) most probable facies compared with the facies log from the discovery well. Two-way traveltime (TWT).

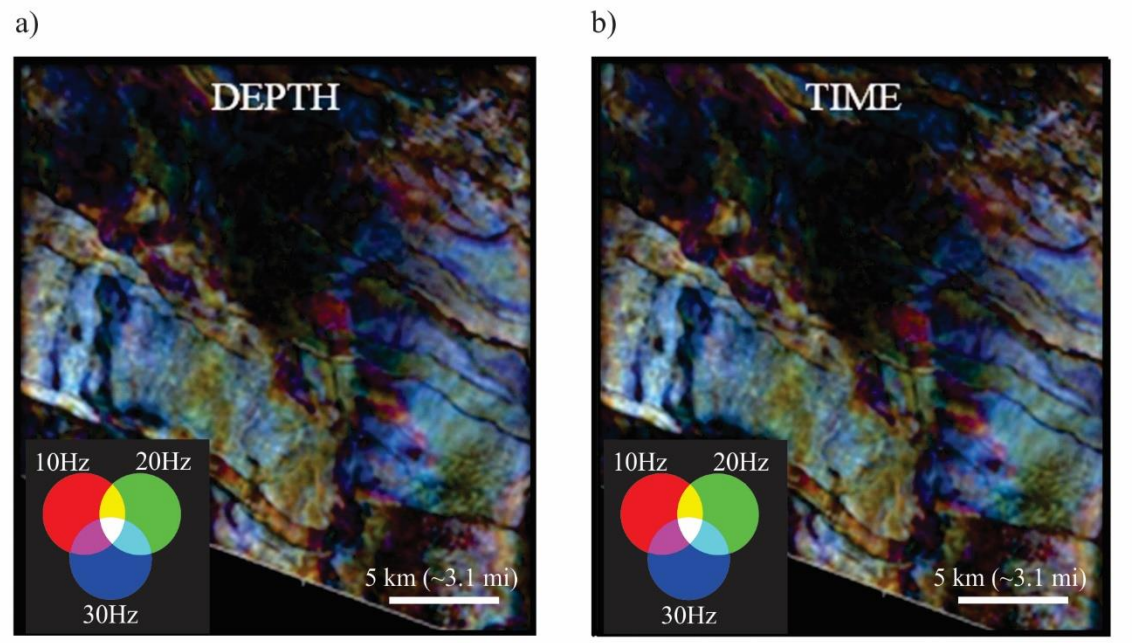

Figure 10: Quality control comparison of spectral decomposition RGB blends in the depth (a) and time (b) domains from a horizon slice.

These spectral decomposition RGB blends are a mix of three attributes, the differences in frequencies and magnitude of which are associated with primary colors. Color variation represents frequency changes, whereas brightness represents changes in amplitude (strong brightness can mean strong positive or negative amplitudes).

The spectral decomposition RGB blends revealed that the profile at the discovery well is quite different from the appraisal well location. According to elastic inversion interpretations, the appraisal well would be a good place to find good-quality sandstones because it has the same characteristics as the discovery well location, but the spectral decomposition RGB blends suggest otherwise because they indicate differences between the two well locations (Figure 11a). The region at the discovery well is brighter and has a purple color, resulting from a mixture of 10 and 30 Hz frequencies, interpreted to be indicative of cleaner sandstones (Figure 11b). As for the region at the appraisal well more opaque green color can be seen, resulting from dominance of the 20 Hz frequency, which could indicate shalier sandstone facies in the appraisal well (Figure 11c). Therefore, the results from spectral decomposition analysis indicate that the appraisal well location had a high probability for finding non-reservoir facies. The seismic facies classification results can be observed in an arbitrary line through the two wells in Figure 12 and compared to well data in Figure 13a and 13b. Porosity and gamma ray logs were used to qualitatively interpret each class, and since the higher porosity and lower gamma ray

(related to shale content) values indicate the best reservoirs classes, the analyzed interval was discriminated into: very good reservoir for class 1 (green), good for class 2 (yellow), moderate for class 3 (purple), poor for class 4 (light blue), and very poor for class 5 (red).

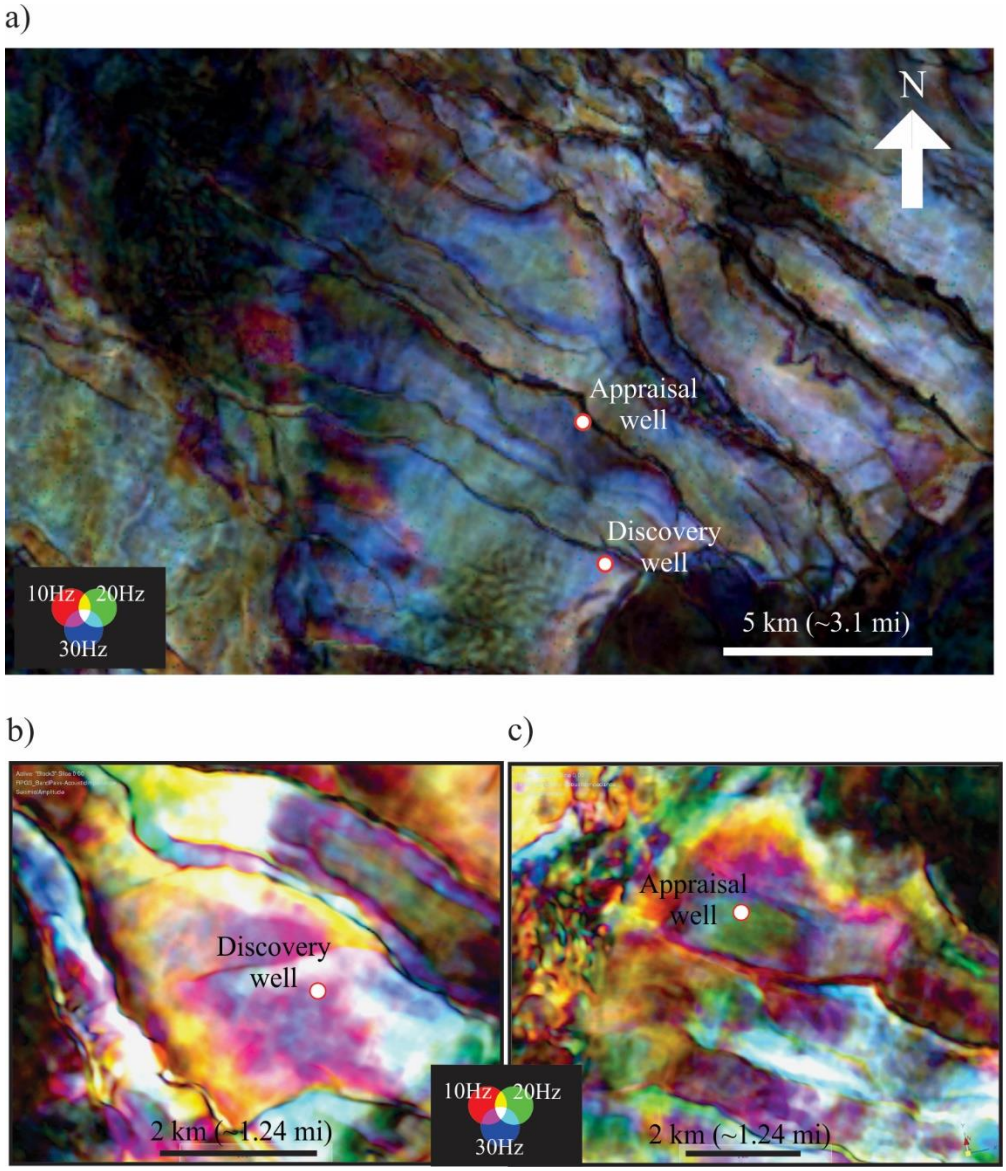

Figure 11: Enhanced view of the spectral decomposition RGB blend for (a) both the discovery and appraisal wells in the study area, (b) zooming in the discovery well (c) zooming in appraisal well.

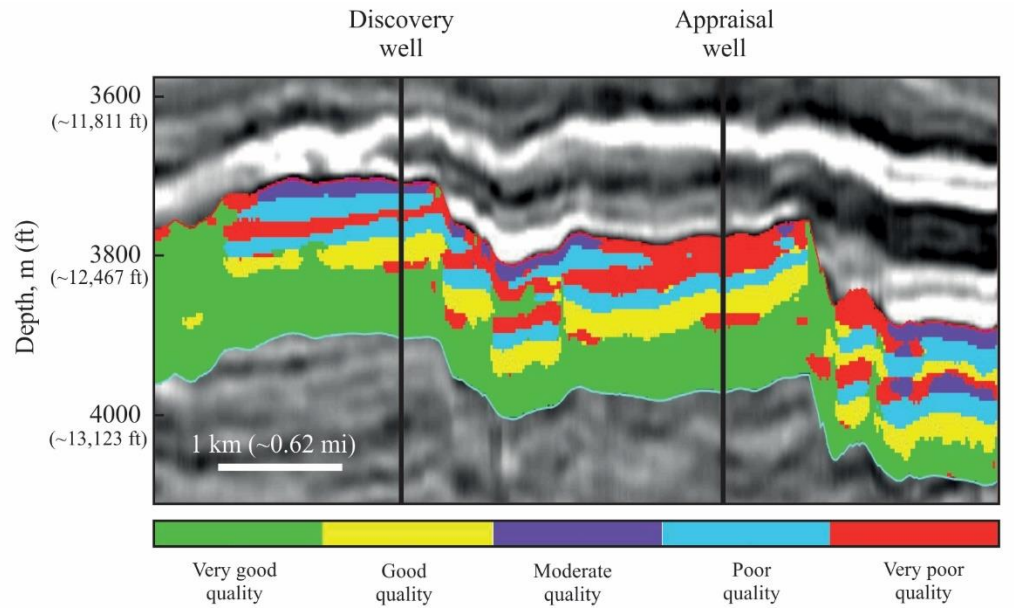

Figure 12: Section view of an arbitrary line crossing the discovery and appraisal wells of seismic facies classification results.

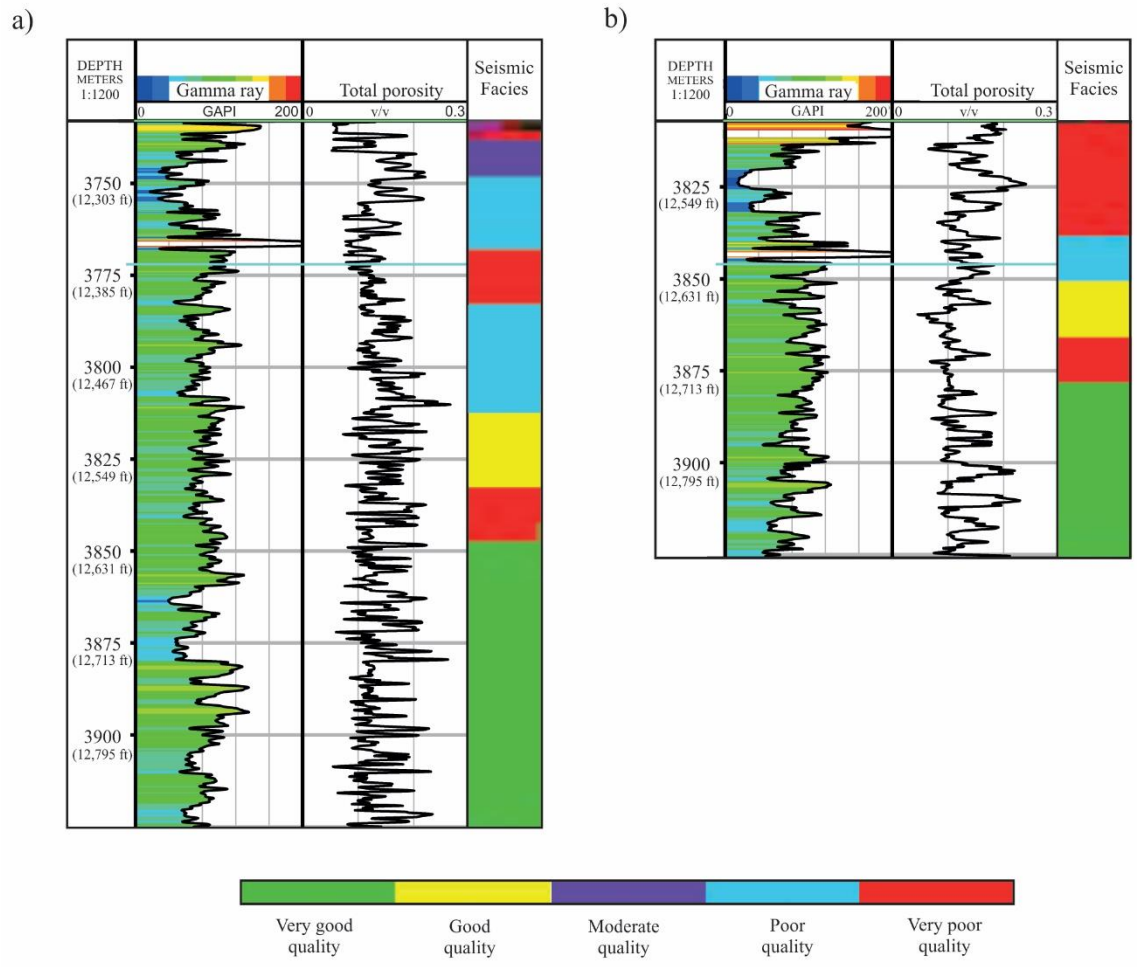

Figure 13: Gamma ray and total porosity logs versus seismic facies classification at the discovery well (a) and at the appraisal well (b) locations.

Predictions about the appraisal well in the seismic facies classification process were performed using only information from the discovery well. The discovery well is in a better location than the proposed appraisal well, because the upper layer in the appraisal well is categorized as class 5 meaning very poor quality compared to the discovery well. These results are consistent with the spectral decomposition results.

After drilling the appraisal well, its porosity and gamma ray logs (Figure 13b) were also compared to the seismic facies classification results. This comparison confirmed that the seismic classification and spectral decomposition analysis were accurate because well log information from the appraisal well revealed the upper part of the well to be shalier hence possessing poorer quality reservoirs compared to the discovery well.

5. Introduction: Carbonate Environment

Brazil has been producing oil from pre-salt carbonate reservoirs over the past decade. Recently, these reservoirs attained an incredible output of just over 1.7 million barrels of oil equivalent per day (boepd), representing more than half of the country's daily production and demonstrating the importance of these carbonate reservoirs to Brazil. However, it is tremendously challenging to map and characterize these carbonate reservoirs given their considerable spatial heterogeneity, complex pore systems and often ambiguous seismic responses.

Burgess et al. (2013) defined criteria for discriminating different carbonate features in a seismic image that involve: regional constraints, analysis of basic seismic geometries, and analyses of geophysical details and finer-scale seismic geometries. For the purpose of this work, we adopted analyses of seismic geometries and geophysical details, as well as amplitude anomalies and the behavior of frequencies in the reservoir interval, together with the high density of faults and fractures, to define carbonate features, many of which were assessed at a sub-seismic scale (Wright and Rodriguez, 2018).

Here, we propose a workflow for identifying and characterizing carbonate mounds in the Brazilian pre-salt zone using a combination of hybrid spectral decomposition (HSD) together with geometrical attributes and curvature and coherence attributes. For this work, we use the term “carbonate mounds” to describe almost conical carbonate bodies of pronounced relief that are often difficult to map seismically due to their ambiguous limits and internal low amplitude reflectors, but that exhibit excellent reservoir quality both in terms of matrix and associated fracturing and that have been successfully drilled, evaluated and tested. It is beyond the scope of this work to interpret these features further or to establish their depositional environment. For a broader perception of the many interpretations of these pre-salt carbonates we suggest, amongst others, the works of Arienti et al. (2018) on Barra Velha Formation depositional systems, Buckley et al. (2015) on early Cretaceous lacustrine carbonate platforms, Wright and Barnet (2017) on depositional models for the pre-salt Barra Velha Formation, and Wright and Rodriguez (2018) on depositional interpretations of pre-salt environments and their links to seismic facies. Our workflow is focused on characterizing seismic facies and their relationship to present-day reservoir quality, which we believe can be applied and

adjusted to different settings within the Brazilian pre-salt sequence. Our intent is to detail a workflow that can facilitate mapping of present-day good reservoir quality carbonate mound geometries to enable their characterization from a seismic perspective and to allow assessment of their spatial distribution for the purposes of reservoir modeling during exploration and appraisal stages.

Seismic attenuation can greatly affect the quality of seismic signals perpetuated at considerable depths (Lupinacci and Oliveira, 2015; Yuan et al., 2017). Consequently, mapping carbonate mounds in the Brazilian pre-salt fields, which lie at depths ranging between 5,000 m and 6,000 m and below an approximately 2,000 m thick layer of salt, is a major challenge for geoscientists because of low seismic illumination and low amplitude anomalies, low impedance, and the high fault and fracture density that are characteristic of these geological features. It is difficult to identify and delineate such features in these pre-salt fields using only seismic data because of the complexity of the seismic image generated and the absence of impedance contrast between the reservoir and adjacent sealing facies (Zheng et al., 2007).

Despite many criteria for presalt seismic data having already been defined, we consider in this study a general information about the acquisition and processing of such data is essential to understanding its ambiguities and limitations its carries. Furthermore, since seismic data can be contaminated by random and coherent noise arising from data acquisition or complex geology that can bias results even after data processing and migration (Chopra and Marfurt, 2007), data preconditioning is crucial to obtain good results (Lupinacci et al., 2017).

With respect to carbonate reservoir characterization, seismic facies analysis is increasingly seen as an effective way of estimating reservoir properties (Matos et al., 2007), combining different seismic attributes through pattern recognition algorithms such as seismic multi-attributes analysis (Rongchang et al., 2017) to identify, for example, lateral changes in a reservoir. Seismic attributes are important tools for reservoir characterization that can help to visually enhance or quantify features of interest (Chopra and Marfurt, 2007). However, selection of seismic attributes for analysis should be made with caution so as not to propagate false interpretations.

Curvature and coherence attributes can be used together in seismic multi-attributes analyses to increase the reliability of this type of geological analysis. The curvature attribute describes how bent a curve is at a point along its length (Roberts, 2001), focusing

on changes in shape. This attribute is a good predictor of faults, as well as anticline and syncline structures (Klein et al., 2008), as it is not affected by variation in amplitude related to changes in lithology and fluid. The coherence cube attribute - a measure of the similarity between neighboring seismic traces in three dimensions - has been used since 1995 (Bahorich and Farmer, 1995) as a powerful seismic interpretation tool for imaging geological discontinuities such as faults and fractures, which are recurrently associated with carbonate mound features in this study area. However, many ways of calculating coherence can be implemented. Here, we applied the eigenvalue-coherence algorithm (Gersztenkorn and Marfurt et al., 1999), which uses several adjacent traces within a local window to estimate discontinuity for each sample.

Spectral decomposition is another widely used attribute for identifying seismic patterns. It can represent the seismic trace in a frequency domain or in sub-bands of frequencies. It can be used to identify subtle thickness variations and discontinuities, as well as to predict bedding thicknesses (e.g. Partyka et al., 1999). Spectral decomposition can also be used to identify low-frequency shadow, which may indicate the presence of hydrocarbons (Sun et al., 2002; Wang, 2007) or as in this study, to identify good quality reservoirs upon calibration by the well log porosity response.

Additionally, a frequency bandwidth related to seismic facies can be selected from a spectral decomposition analysis, so a specific amplitude range can be isolated that represents a reservoir anomaly (termed hybrid spectral decomposition, HSD) (Jesus et al., 2017).

Pattern recognition and classification of seismic features is fundamental to seismic data interpretation (Zhao et al., 2015), so uniting different criteria through several seismic attributes and establishing seismic facies classes is an excellent approach for isolating reservoirs of good quality in pre-salt carbonate mounds from shale or tight zones (non-reservoir).

We propose a workflow for identifying and characterizing carbonate mounds in the Brazilian pre-salt zone using a combination of HSD with curvature and coherence geometric attributes. We chose those attributes because of their ability to provide useful geological information and used them to generate a seismic facies classification to specifically identify good quality reservoirs in carbonate mounds. The extracted geobody was then used as a spatial indicator of the distribution of porosity in the reservoir.

6. Methodology: Article 2

As described in Burgess et al. (2013), there is no clear set of diagnostic criteria for identifying many specific carbonate features, especially in frontier regions. From a geophysical perspective, the Brazilian pre-salt zone is still a frontier area, and given the influence of salt thickness on image quality of seismic data, seismic acquisition and processing details need to be carefully understood prior to performing any proposed methodology for seismic data interpretation.

Our workflow starts with preconditioning of the seismic data (Figure 14) using structural-oriented filtering (SOF) to remove some background noise and preserve fault edges. The SOF volume is then used to generate the curvature attribute. In parallel and to improve overall vertical resolution, an image enhancement is applied to the SOF volume to calculate a coherence cube, which facilitates better identification of the faulted and fractured character of these pre-salt carbonate mounds.

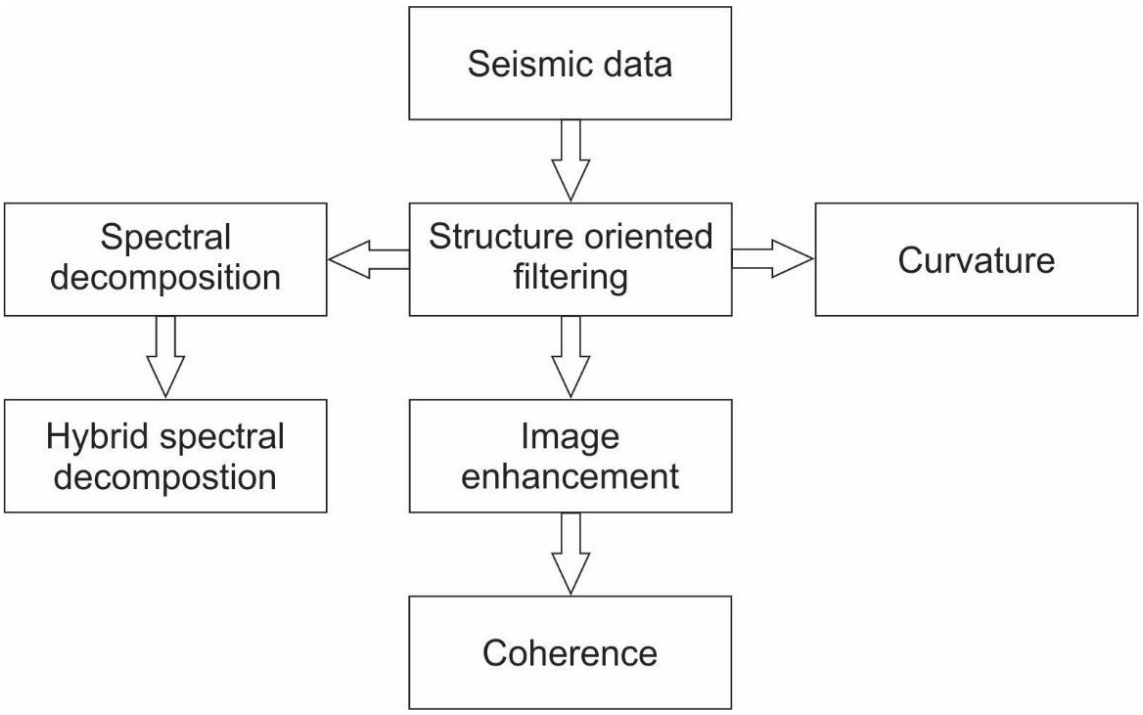

Figure 14: Steps used to calculate the seismic attributes.

We also apply HSD to the SOF volume to identify low amplitude zones, which correspond to areas of good porosity. All these seismic attributes are then combined to classify the seismic facies, which allow us to distinguish the most important facies

representing good reservoir quality carbonate mounds, and to extract a geobody that can then be used as a spatial control for porosity distribution in reservoir modeling.

Our methodology for characterizing carbonate mounds is thus divided into four stages: 1) seismic data acquisition and processing overview; 2) preconditioning of seismic data; 3) calculation of seismic attributes; and 4) classification of seismic facies. We describe these processing stages in detail in the following sections.

6.1. Seismic data acquisition and processing overview

The seismic acquisition was performed in 2013 from a single vessel equipped with 12 streamers, 8,000 m in length, and dual sources. The seismic data was recorded with an azimuth direction of 123º, a sampling rate of 2 ms, and a nominal fold of 80. Seismic acquisition parameters are presented in Table 2.

Table 2: Acquisition parameters from a single vessel.

Acquisition parameters	
Shot interval	25 m
Cell length	6.25 m
Cell width	12.5 m
Line orientation	123° or 303°
Near offset (inline)	150 m
Source numbers	2
Source separation	25 m
Source depth	7 m
Streamer numbers	12
Streamer length	8000 m
Group interval	12.5 m
Group length	12.5 m
Streamer depth	9 m
Streamer separation	50 m

Depth imaging and velocity model building in deep-water environments with complex and large evaporated layers is challenging for seismic illumination. These seismic acquisition parameters are not ideal for seismic illumination of pre-salt reservoirs.

Had the seismic data been acquired as broadband, we could have applied a more efficient seismic processing.

The initial velocity model building (VMB) was rendered on legacy data to obtain a more realistic and geologically relevant outcome by first applying an isotropic model for the initial step and then deriving a tilted transversal isotropic (TTI) model from the tomographic data along with the seismic inversion (Bakulin et al., 2010). To decrease the well-to-seismic mistie, we updated the anisotropy models based on the well markers. Another important strategy we adopted for the VMB was to divide the salt layer using intermediate horizons that separated stratified salt from homogeneous salt. The background starting salt velocity for the tomography was 4,500 m/s, and then we applied a weighted mask to guide the tomography and produce a stronger update in the stratified salt layer. This strategy made it possible to establish a more precise velocity model for the pre-salt zone.

6.2. Preconditioning of seismic data

According to Höecker and Fehmers (2002), three premises are required to apply filters successfully on post-stack seismic data: orientation analysis, edge detection, and smoothing with edge preservation. Furthermore, considering the criteria we adopted in this case study (which include amplitude, frequency anomalies, geometry, and fault and fracture density), application of SOF should guarantee that the quality of the data improves without having to change the criteria.

In order to improve the quality of the seismic data contaminated with background noise, we applied SOF and image enhancement (Figure 15 b and c) to precondition the seismic data (Qi et al., 2014). Pre-conditioning should be concentrated in the region of interest. The aim of SOF is to improve the lateral continuity of the seismic reflector and increase the signal-to-noise ratio (S/N). The SOF algorithm applies volumetric dip and azimuth calculations to avoid smearing of faults, fractures and other discontinuities using an overlapping window method (Marfurt, 2006). We used the SOF output to calculate an image enhancement through increasing frequency bandwidth (Bruce and Caldwell, 2003), thereby bolstering weak frequencies to reduce the effect of attenuation (Figure 15c). This step could be considered a type of spectral enhancement, the objective of which was to improve seismic resolution by increasing the frequency bandwidth. This process

does not create new frequencies, it only enhances the contribution of some frequencies existing within the seismic data to better define reservoir architecture.

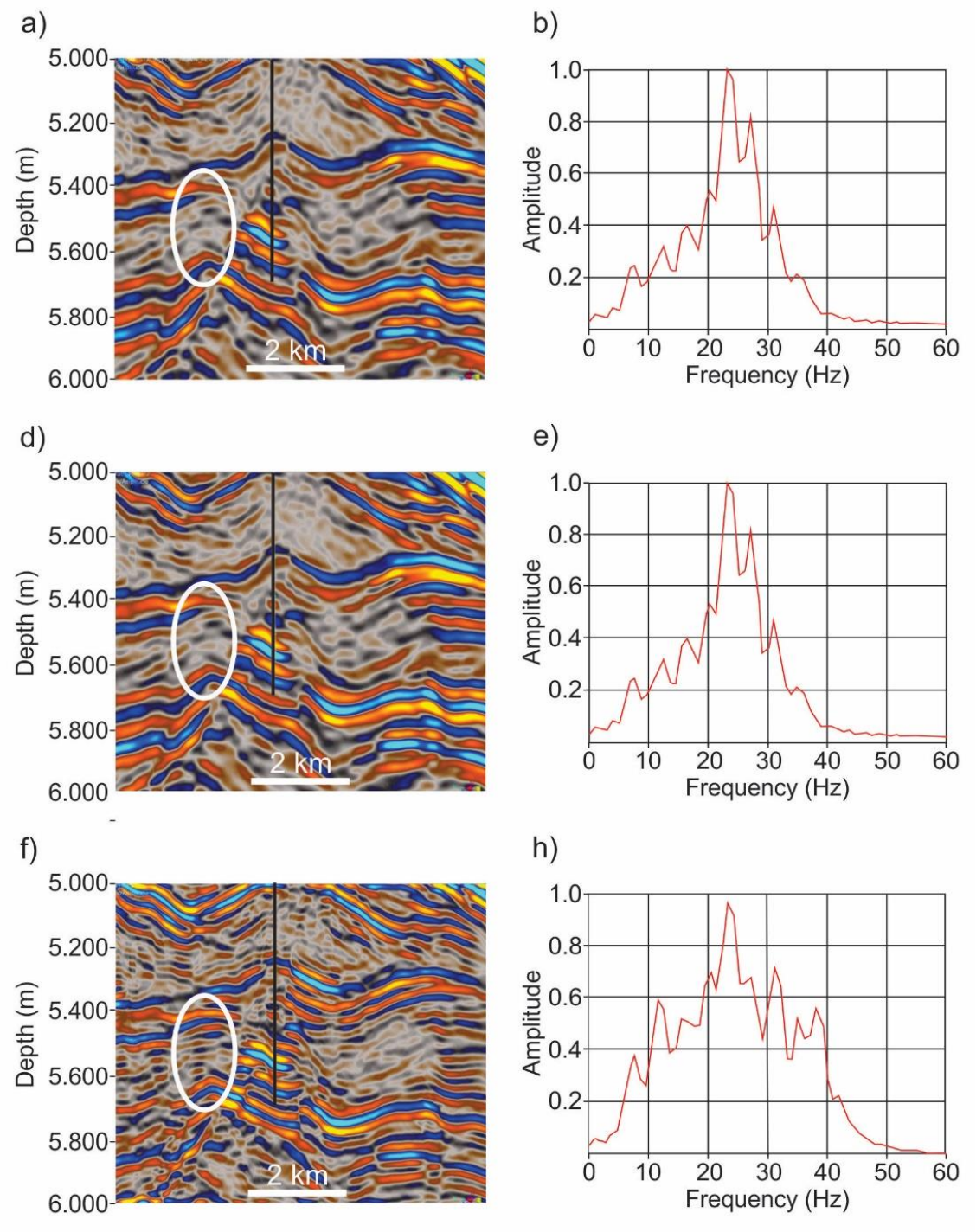

Figure 15: Preconditioning. (a) Input; (b) SOF; (c) Imaging enhancement.

6.3. Calculation of seismic attributes

The seismic attributes were calculated after SOF and image enhancement. The curvature and spectral decomposition attributes were generated directly from SOF. The

coherence attribute was derived from the image enhancement step. The hybrid spectral decomposition (HSD) was obtained from the spectral decomposition step. The steps for calculating the seismic attributes are shown in Figure 14.

The curvature attribute describes how a surface deviates from being planar (Figure 16). Basically, it measures subtle lateral and vertical changes in dip that are often dominated by strong localized deformation; for example, carbonate reefs on 20^0 dipping surfaces can present the same curvature anomaly as a carbonate reef on a flat surface (Chopra and Marfurt, 2007). In this case study, several curvature attributes were tested, including the most positive, most negative, and dip curvatures. We found that dip curvatures, which are acquired by extracting the curvature in the direction of maximum dip, presented the best result. Volume curvature attributes can enhance seismic resolution, providing more insight into fault delineation and aiding in the prediction of fractures and their orientations (Roberts, 2001; Chopra and Marfurt, 2007). The curvature attribute is very susceptible to noise, so we calculated it after SOF.

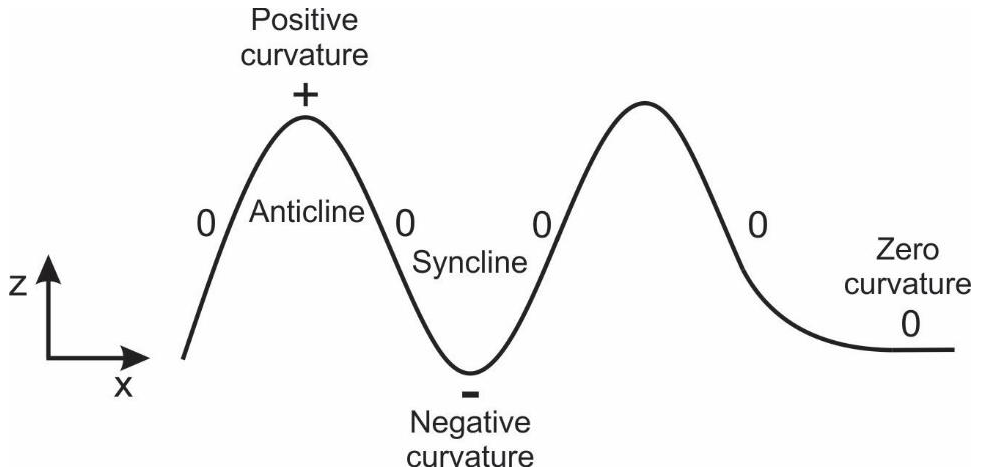

Figure 16: Curvature attribute in two dimensions, indicating that this attribute is positive in an anticline, negative in a syncline, and zero in a flat or dipping plane.

The coherence attribute requires a central trace as a reference to make correlations between neighboring seismic traces using a vertical analysis window (Figure 17). Geologically, highly coherent seismic traces or waveforms indicate a laterally continuous lithology. Abrupt changes in waveform can indicate faults and fractures in the sediments (Chopra and Marfurt, 2007). According several tests, it was possible to see that the difference between the curvature calculation results before and after image enhancement. It was possible to see that there is the risk of boost up some noise and this attribute is very sentitive to noise level. And coherence shows to be more effective after improvement of

the resolution. We used the coherence attribute to search along structural dips, since it helps to reveal true edges.

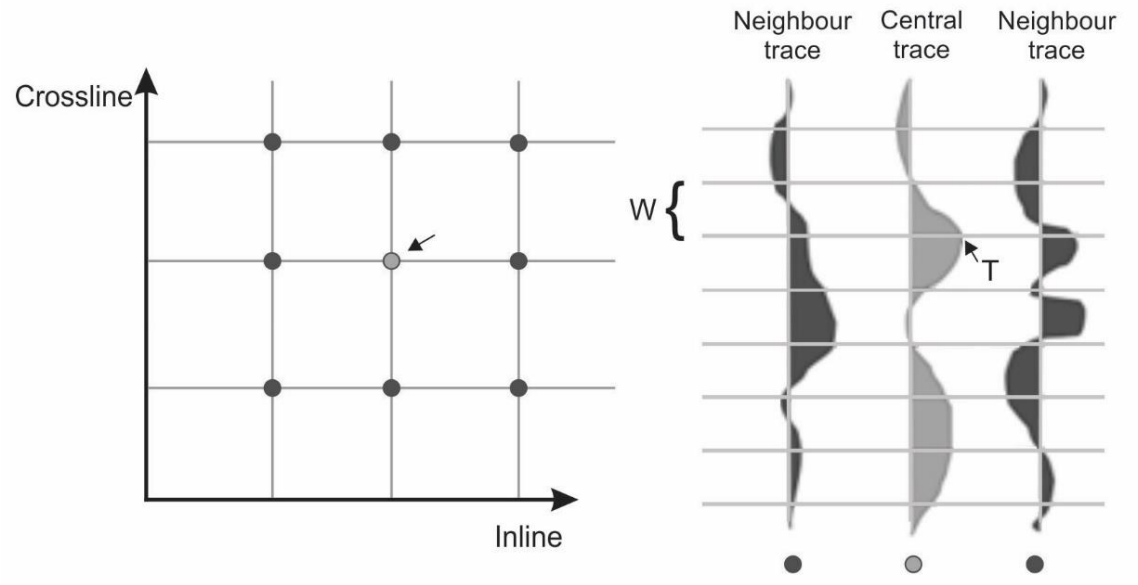

Figure 17: Spatial (or multitrace) analysis windows used to calculate the coherence attribute (W is defined as the vertical analysis window for time T).

After we analyzed the dominant frequency and identified the frequency bandwidth that best represents the target, we used HSD to decompose the seismic data into frequency bands. This frequency bandwidth is selected to calculate the envelope attribute from which a specific amplitude range is isolated (Jesus et al., 2017). We obtained the HSD parameters after SOF application to maintain the proportionality of the amplitude and thereby preserve the reservoir anomalies. In order to achieve an optimized hybrid spectral decomposition for the area of interest, two steps are required: a sensitivity study (Stage 1); and an isolation study of both frequency ranges and representative amplitudes (Stage 2).

Stage 1: For the sensitivity study, performed between the top and base of the reservoir of interest, we generated a dominant frequency attribute (Figure 18a) and selected the dominant frequency that best represented the reservoir interval. By analyzing the dominant frequency map at well locations 1, 2 and 3, we identified the dominant frequency as being approximately 8 Hz. Also, as part of our sensitivity study and using the same interval, we generated a root mean square amplitude map to identify low amplitude zones, which is a recurring characteristic of pre-salt carbonate mounds. As illustrated in Figure 18b, all wells except for well 4 are in low amplitude zones.

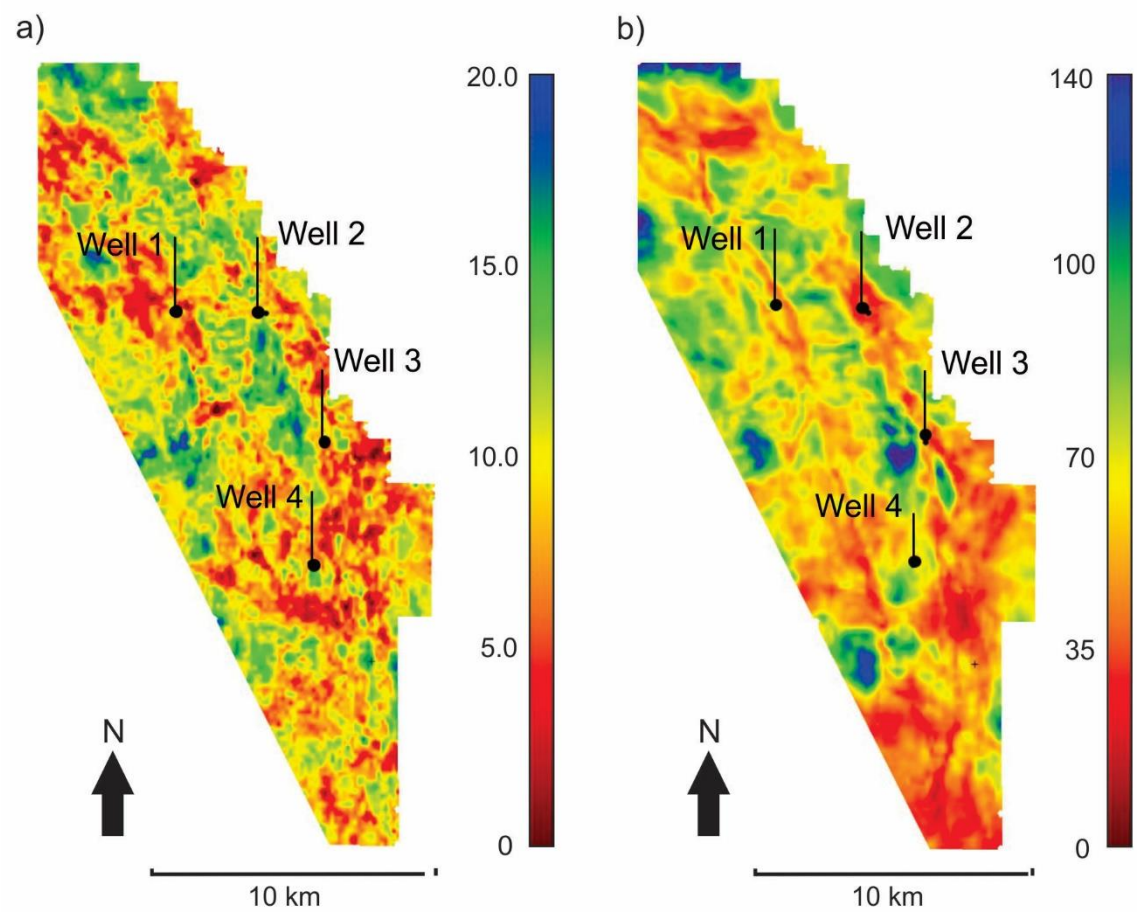

Figure 18: Dominant frequency. (a) Root mean square amplitude; (b) maps.

Stage 2: After our sensitivity study had revealed the frequency best representing the interval of interest and we had identified the respective low amplitude zones through Stage 1, we could isolate the frequency and amplitude ranges by applying a Short-Time Fourier Transform (STFT) with a Hanning window for spectral decomposition of the SOF volume (Figure 15) and decompose the seismic data into frequency sub-bands. By knowing the representative frequency and well outcomes at the best well locations (wells 1, 2 and 3) and identifying the low amplitude zones for the pre-salt carbonate mounds being investigated, we could isolate the frequency and amplitude associated with the carbonate mounds by selecting a dominant frequency sub-band of 8 Hz and then calculating an envelope attribute for this sub-band. To define the interval for the envelope that represents these pre-salt carbonate mounds, it was necessary to also use the acoustic impedance volume, which assumes a low impedance occurrence in the mound zones represented by wells 1, 2 and 3 (whereas well 4 was defined as non-reservoir).

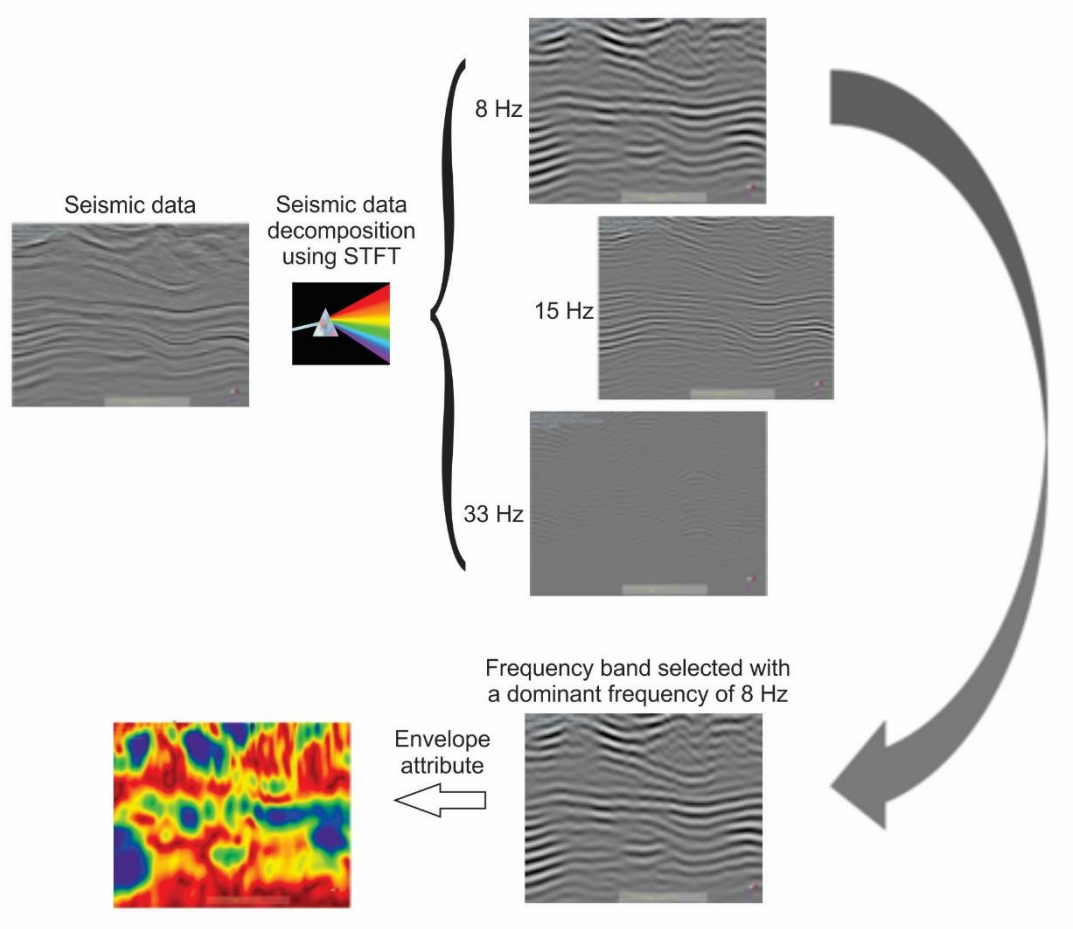

Figure 19: Schematic of stage 2 for optimization and application of HSD (Hybrid Spectral Decomposition). First, the STFT (Short Time Fourier Transform) is applied and a frequency band is selected. Then the envelope attribute is calculated.

As well 4 also presented a high value for the 8 Hz envelope, we established a cutoff to effectively isolate the carbonate mounds by combining the 8 Hz dominant frequency with the acoustic impedance volume representing a low impedance for the carbonate mounds. Where both the 8 Hz envelope and acoustic impedance presented low values, the area was considered a carbonate mound, but when only the envelope attribute value was low, the area was considered a non-reservoir (Table 3). We applied a maximum cutoff value of 0.27 for the envelope attribute to discriminate between reservoirs and non-reservoirs.

Table 3: Correlation between envelope and acoustic impedance.

Attributes	Reservoir (mounds)	Non-reservoir (shale)
Envelope	Low value	High value
Acoustic impedance	Low value	Low value

Finally, the following script was applied to the envelope attribute for 8 Hz as the dominant frequency (spectral decomposition) to generate the hybrid spectral decomposition:

HSD = IF Envelope Value <= 540 THEN Envelope = Envelope ELSE Envelope = 541;

Accordingly, if the envelope value was less than or equal to 540 then the value was retained (to represent reservoirs), otherwise the standard value of 541 was assigned (representing non-reservoirs). The spectral and hybrid spectral decompositions for the top reservoir horizon are shown in Figure 20. A southeast to northwest trend of low amplitude passing through wells 2 and 3 can be seen in Figure 20a, which can be associated with the carbonate mounds. Figure 20b reveals that HSD was better than spectral decomposition in identifying the main low amplitude trend corresponding to carbonate mounds (wells 2 and 3).

Figure 21 shows the main quality control of HSD, where pseudo-log data from HSD was extracted at each well location (wells 1, 2, 3 and 4) and compared with the total porosity log rescaled to seismic output. The quality control showed good correlation between HSD pseudo-log and total porosity, so for low HSD values there is an inversely proportional high value for total porosity. This outcome increases the confidence in our HSD.

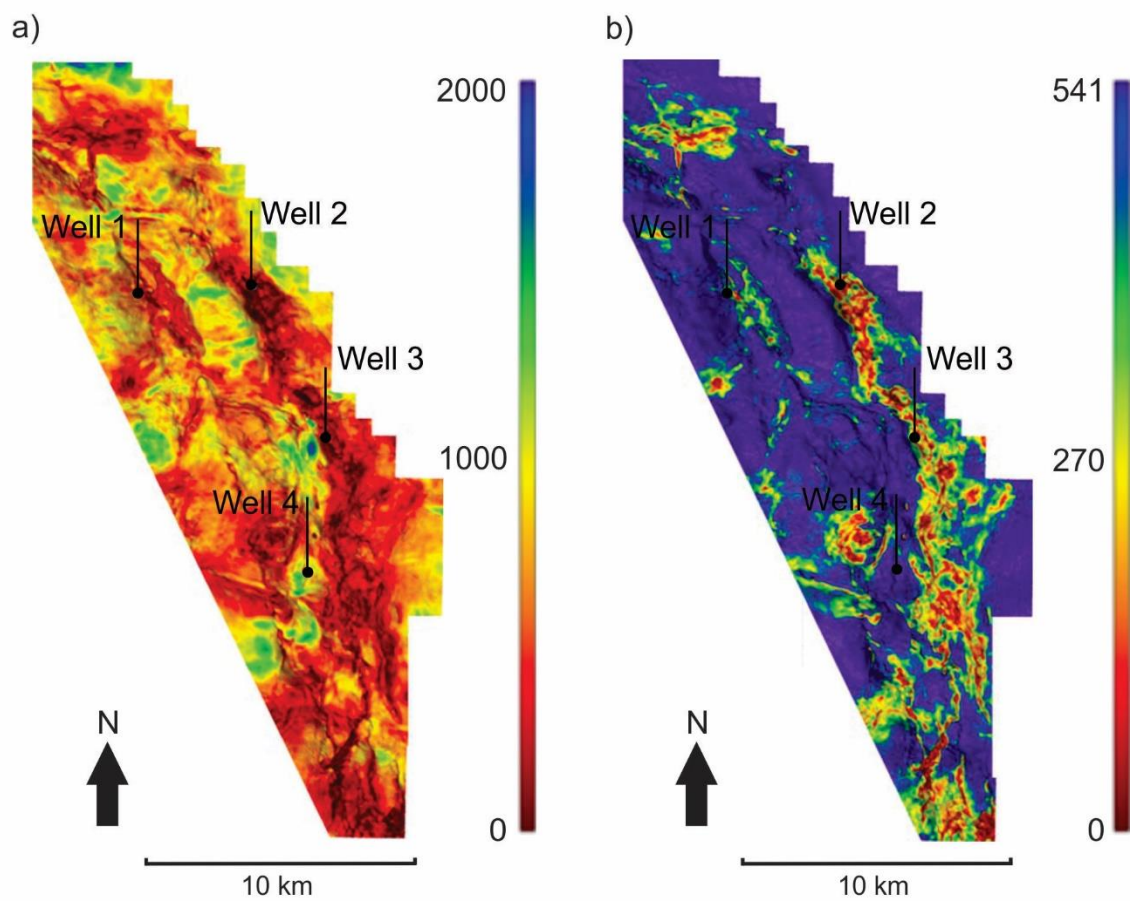

Figure 20: Spectral Decomposition (a), Hybrid Spectral Decomposition (b).

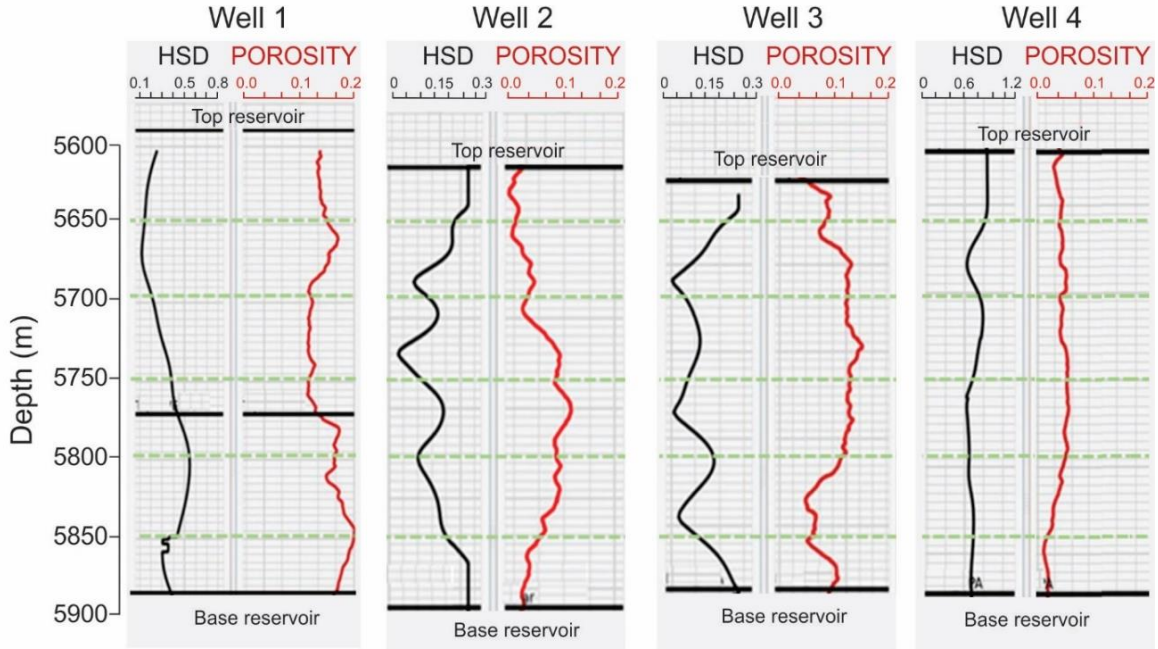

Figure 21: The hybrid spectral decomposition pseudo log (black) and the porosity log (red) are well correlated (inversely). These logs were used as a quality control.

6.4. Seismic facies classification

Seismic facies can be defined as a group of seismic responses with characteristics that distinctly differ from other facies (John et al., 2008). According to Farzadi (2006), a 3D multi-attribute seismic facies classification helps to identify lithofacies and geometric variations within carbonate features.

Our selection of the seismic attributes is based on the geological information that each attribute could provide to identify the good reservoir quality geometries we sought. The curvature attribute was useful for identifying the fractures and fault zones based on the curvature and discontinuities in the seismic reflector (Figure 22a). The coherence attribute also proved useful for identifying high-density fault zones in the carbonate reservoir (Figure 22b). We apply HSD in our workflow because pre-salt carbonate mounds typically exhibit low amplitudes due to fractures increasing their porosity. All these attributes (curvature, coherence and HSD) are then combined for seismic facies classification, which is constrained from the top to the base of the reservoir.

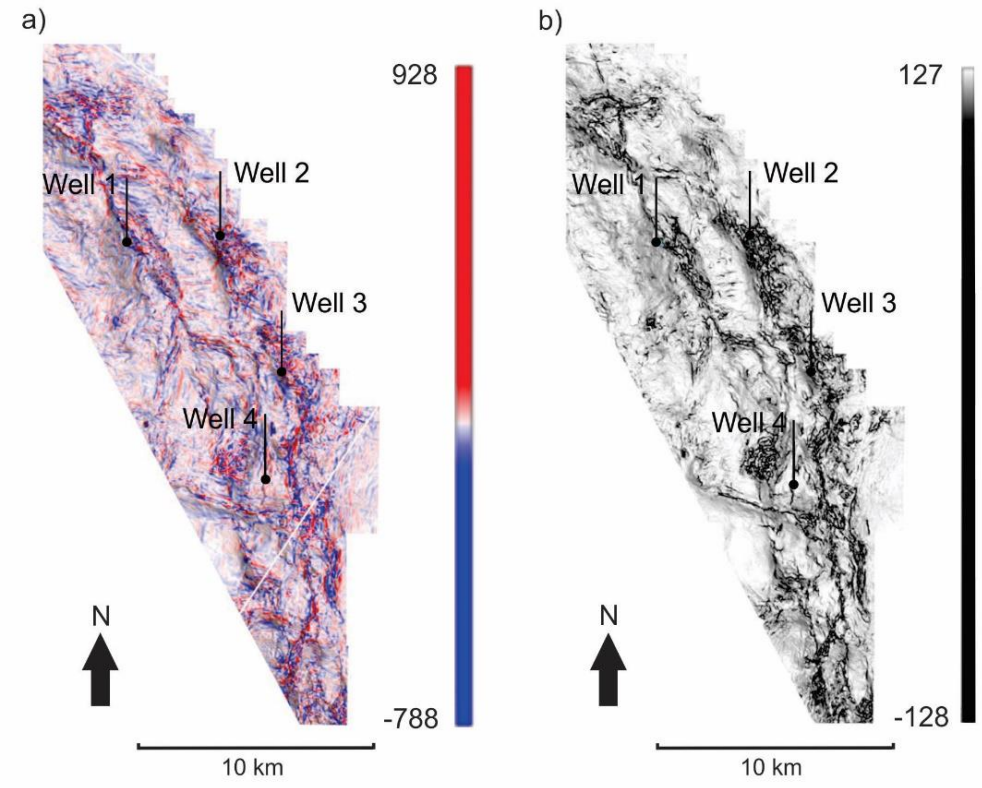

Figure 22: Curvature (a) and coherence (b) attributes applied to the structural map of the top of the reservoir, revealing faults and fracture zones around the wells.

The clustering technique that we use is unsupervised, which aims to partition the dataset into clusters without a priori information concerning the membership in a given cluster of a sample input (Xu and Wunsch, 2005). We employ a neural network as the algorithm for this unsupervised analysis because a priori tests show that it generates a partition with gradual changes in seismic facies patterns.

The input data are highly dimensional and voluminous, which can be problematic for seismic facies classification. Redundancy and excess dimensionality can be reduced by principal component analysis (PCA) (Zhao et al., 2015), through which the input dataset is projected into a lower dimensional space formed by a subset of the highest variance principal components (Bishop, 1995).

Principal component analysis (PCA) and self-organizing maps (SOM) represent multi-attributes analyses that have proven excellent approaches for pattern recognition during seismic interpretation and reservoir characterization (Roden et al., 2015; Zhao et al., 2015). PCA can be used to convert statistical relationships among multidimensional data into simple, geometric relationships and to organize a dataset of seismic attributes into a geometric SOM (Matos et al., 2007), producing a partition with changing patterns of seismic facies. In this work, we apply PCA with three components. To do this, we organized the model facies into a sequence of reference vectors in one dimension. The main purpose of PCA in this case is to assess the relative weights between curvature, coherence and HSD and thereby minimize redundancy. An optimal facies model is established through an iterative adaptation process. The clustering process starts by first specifying arbitrary nodes. Then a sample input is chosen and mapped to the closest node. The optimal facies model and its adjacent neighbors are adjusted towards the sample input and this step is repeated for 65 iterations so that the optimal facies model along with its closest neighbors become more like the selected input sample.

The seismic facies (Figure 23) we obtained in this work were generated using the following parameters: five classes, PCA with three components, and an unsupervised neural network method. The number of classes is defined empirically through what we term a "360º approach" (Figure 24) that consists of the following iterative loops: 1) obtain all seismic attributes and analyze them in order to see if they honor the defined criteria; 2) perform quality control using well information (in this work, we compare total porosity with HSD); 3) run unsupervised seismic facies classification; 4) select representative facies with features of good reservoir quality carbonate mounds and observe the resultant

geobody extraction; 5) crosscheck the geobody distribution versus Hydraulic Flow Unit (HFU), where HFU 2 and 3 means there is no flow and HFU 4 means there is flow ; and 6) finish the process if the results are consistent with the well log response and, if not, re-run it but change key parameters (in our case, we changed the HSD cutoffs and the number of seismic facies).

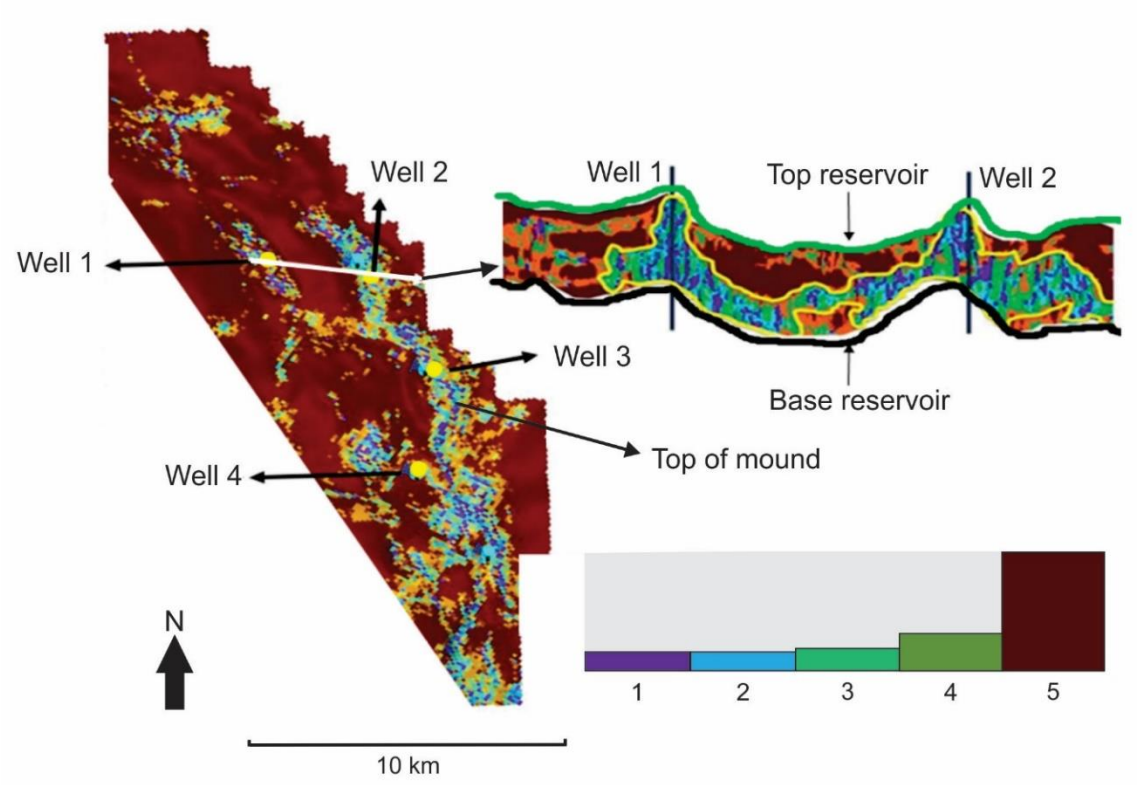

Figure 23: Seismic facies. Structural map of the top of the reservoir, highlighting the carbonate mounds.

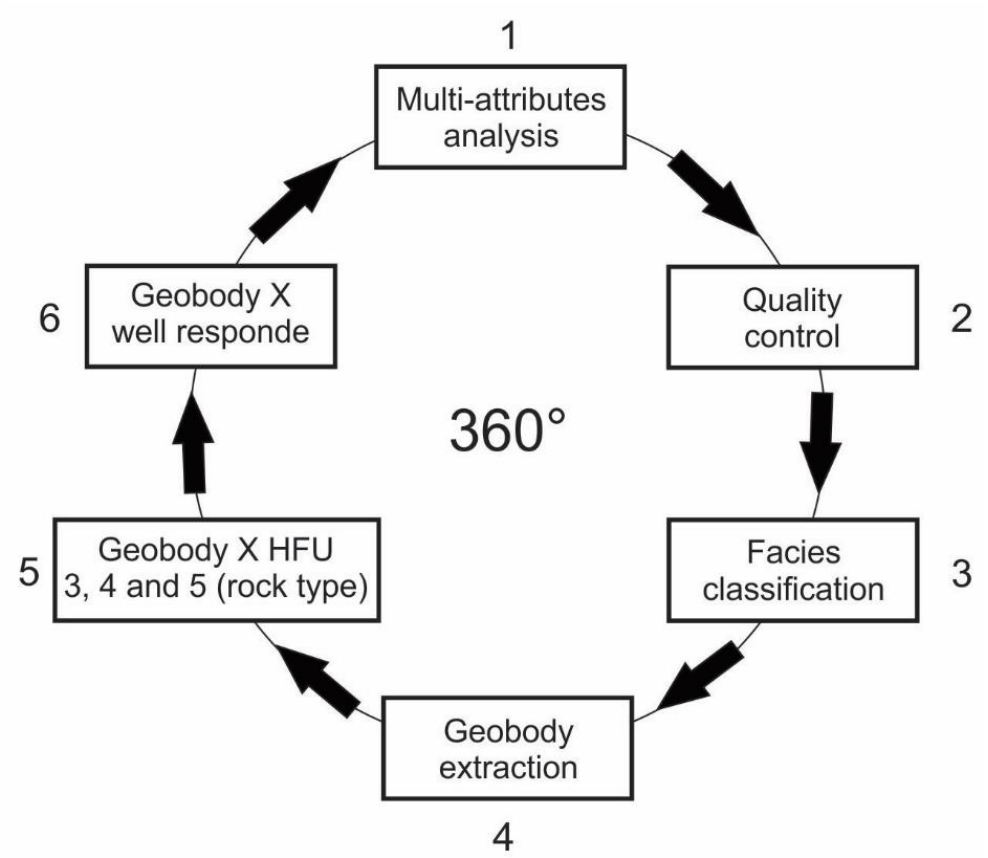

Figure 24: Illustration of our “360º approach” applied in this work.

7. Results and Discussions: Article 2

The outcomes of applying the curvature and coherence attributes to the structural map of the top of the reservoir are shown in Figure 22 (a and b). Low coherence values and high variations in curvature were found around carbonate mounds, indicating a high density of faults and fracture zones.

We use the wells as a quality control to interpret the results of our HSD. We first calculate pseudo logs of the HSD with a central frequency of 8 Hz that behaved similarly to the background model for seismic inversion. Inverse correlations between the pseudo logs of the HSD and porosity for each well are presented in quality control (Figure 21). Well 4, which is in a clay zone, presents low HSD values.

Geometric attributes (curvature and coherence) were used to identify zones with a high density of faults and fractures, typical of carbonate mounds, for the seismic facies classification. Those attributes are also combined with the HSD data. We chose five classes of seismic facies, and a facies map indicating reservoir heterogeneities is provided in Figure 23. This map reveals facies connectivity. Facies 1-3 were identified in our 360º approach as carbonate mounds with high porosity and a high density of fractures, representing the best reservoirs. In this work, we consider classes 4 and 5 as non-reservoirs in terms of their quality. Figure 25 shows the extracted geobody of Facies 1-3 classified as good reservoir quality carbonate mounds. It is noteworthy that wells 2 and 3 are in this geobody, whereas wells 1 and 4 are in an area not identified as a carbonate mound, corroborating the well log response.

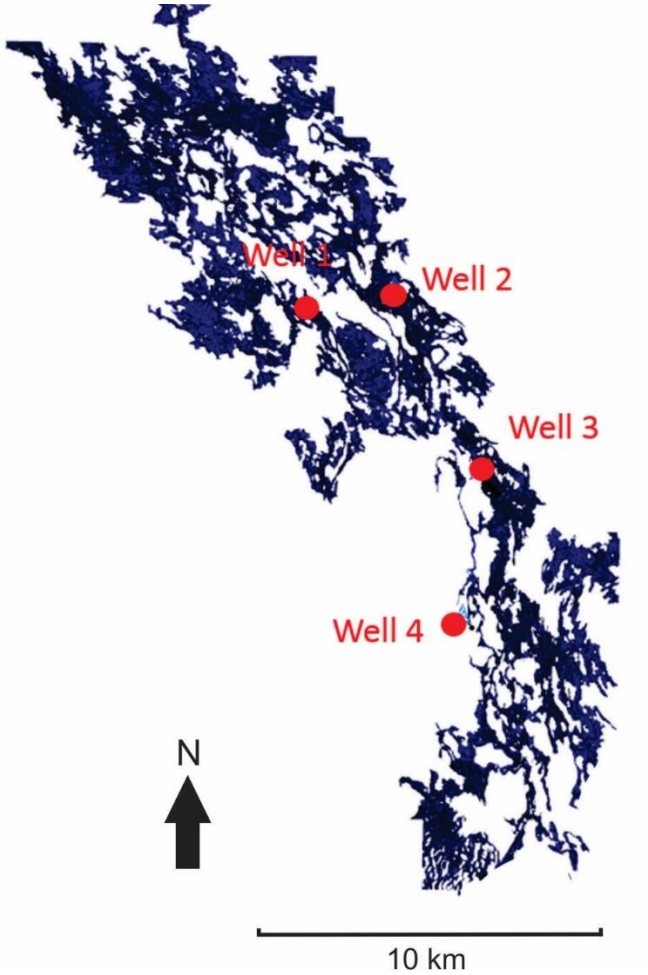

Figure 25: Geobody of carbonate mounds extracted from seismic facies classification.

8. Conclusions

8.1. Conclusions of the Article 1

The preconditioning of seismic data and optimization approach used were critical to guaranteeing that the target zone was accurately represented in the spectral decomposition method. Elastic inversion results indicated that the discovery and appraisal well locations had good quality sandstones as reservoir facies. However, the spectral decomposition analysis indicated otherwise because it showed different signals at the well locations. These differences were interpreted as an indication of cleaner sandstones at the discovery well and shalier sandstones at the appraisal well. Seismic facies classification was achieved using a combination of acoustic inversion, coherence, dominant frequency and spectral decomposition attributes, resulting in a satisfactory outcome, exhibiting a good correlation with porosity and gamma ray well log data. Again, these results showed that the appraisal well had a poorer reservoir quality when compared to the discovery well, as predicted by the spectral decomposition. The proposed methodology would have allowed the prediction of reservoir potential before the appraisal well was drilled, which was confirmed by drilling, thus proving the effectiveness of the proposed approach in reducing exploration risk.

8.2. Conclusion of the Article 2

The proposed workflow proved efficient in identifying good reservoir quality carbonate mounds within the complex environment of the Brazilian presalt zone. The coherence and curvature attributes were useful tools for identifying faults and fracture zones, high densities of which represent one of the most important characteristics of carbonate mounds. Because low seismic amplitude is also a typical feature of presalt carbonate mounds, we used HSD that allowed us to discriminate good reservoir quality carbonate mounds from poor reservoir zones (as identified for well 4). Our multiattributes facies classification generated a geologically significant outcome for static modeling, and the extracted geobody was used as an additional spatial indicator of porosity distribution. This workflow has been successfully applied in three other presalt carbonate fields.

References

Addison, P. S., 2002, The Illustrated Wavelet Transform Handbook: Introductory Theory and Applications in Science, Engineering, Medicine and Finance: CRC Press, 368 p.

Arienti, L. M., R. S. Souza, S. Viana, M.A. Cuglieri, R. P. Silva, S. Tonietto, L. Paula, J. A. Gil, 2018, Facies Association, Depositional Systems, and Paleophysiografic Models of the Barra Velha Formation, Pre-Salt Sequence – Santos Basin, Brazil: ACE 2018 Annual Convention & Exhibition, Salt Lake City, Utah.

Avseth, P., T. Mukerji, and G. Mavko, 2005, Quantitative seismic interpretation, applying rock physics to reduce interpretation risk: Cambridge University Press, 376 p.

Bahorich, M., and S. Farmer, 1995, 3D seismic discontinuity for faults and stratigraphic features: The coherence cube: The Leading Edge, **14**, no. 10, 1053–1058, doi: 10.1190/1.1437077.

Bakulin, A., M. Woodward, D. Nichols, K. Osypov, and O. Zdraveva, 2010, Building tilted transversely isotropic depth models using localized anisotropic tomography with well information: GEOPHYSICS, v. 75, no. 4, p. D27–D36, doi:10.1190/1.3453416.

Bredesen, K., E. H. Jensen, T. A. Johansen, and P. Avseth, 2015, Quantitative seismic interpretation using inverse rock physics modelling: Petroleum Geoscience, v. 21, p. 271-284, doi: 10.1144/petgeo2015-006.

Bishop, C. M., 1995, Neural networks for pattern recognition: Oxford University Press.

Bruce, Z. S., and D. H. Caldwell, 2003, A bandwidth enhancement workflow through wavelet analysis: SEG Technical Program Expanded Abstracts 2003, 2012–2015, https://doi.org/10.1190/1.1817725.

Buckley, J. P., D. Bosence, and C. Elders, 2015, Tectonic setting and stratigraphic architecture of an Early Cretaceous lacustrine carbonate platform, Sugar Loaf High, Santos Basin, Brazil: Geological Society, London, Special Publications, **418**, no. 1, 175–191, doi: 10.1144/SP418.13.

Burgess, P. M., P. Winefield, M. Minzoni, C. Elders, 2013, Methods for identification of isolated carbonate buildups from seismic reflection data: AAPG Bulletin, **97**, no.

7, 1071–1098, doi: 10.1306/12051212011.

Castagna, J., and S. Sun, 2006, Comparison of spectral decomposition methods: 75-79 p.

Castagna, J. P., S. Sun, and R. W. Siegfried, 2003, Instantaneous spectral analysis: Detection of low-frequency shadows associated with hydrocarbons: The Leading Edge, v. 22, no. 2, p. 120–127, doi:10.1190/1.1559038.

Chopra, S., and K. J. Marfurt, 2007, Seismic Attribute for Prospect Identification and Reservoir Characterization: SEG Geophysical Developments No. 11, doi: 10.1190/1.9781560801900.

Chopra, S., and K. J. Marfurt, 2007, Structure-oriented Filtering and Image Enhancement, *in* Seismic Attributes for Prospect Identification and Reservoir Characterization: Society of Exploration Geophysicists and European Association of Geoscientists and Engineers, Geophysical Developments Series, p. 187–218, doi:10.1190/1.9781560801900.ch8.

Chopra, S., and K. J. Marfurt, 2014, Churning seismic attributes with principal component analysis, *in* SEG Technical Program Expanded Abstracts 2014: Society of Exploration Geophysicists, p. 2672–2676, doi:10.1190/segam2014-0235.1.

Connolly, P., 1999, Elastic impedance: The Leading Edge, v. 18, no. 4, p. 438–452, doi:10.1190/1.1438307.

Deboeck, G., and T. Kohonen (eds.), 1998, Visual Explorations in Finance: London, Springer London, Springer Finance, 229 p., doi:10.1007/978-1-4471-3913-3.

Du, K., and M. N. S. Swamy, 2014, Neural Networks and Statistical Learning: London, Springer London, 824 p., doi:10.1007/978-1-4471-5571-3.

Farzadi, P., 2006, Seismic facies analysis based on 3d multi-attribute volume classification, Dariyan Formation, SE Persian Gulf: Journal of Petroleum Geology, **29**, no. 2, 159–174, doi: 10.1111/j.1747-5457.2006.00159.x.

Ferreira, D. J. A., W. M. Lupinacci, 2018, An approach for threedimensional quantitative carbonate reservoir characterization in the Pampo field, Campos Basin, offshore Brazil: AAPG Bulletin, v. 102, no. 11, p. 2267–2282, doi: 10.1306/04121817352.

Ferreira, D. J. A., W. M. Lupinacci, I. A. Neves, J. P. R. Zambrini, A. L. Ferrari, L. A. P. Gamboa, M. Olho Azul, 2019, Unsupervised seismic facies classification applied

to a presalt carbonate reservoir, Santos Basin, offshore Brazil. AAPG Bulletin, v. 103, p. 997-1012, doi: 10.1306/10261818055.

Gersztenkorn, A., K. J. Marfurt, 1999, Eigenstructure-based coherence computations as an aid to 3-D structural and stratigraphic mapping: Geophysics, **64**, no. 5, 1468-1479, doi.org/10.1190/1.1444651.

Grana, D., 2016, Rock Physics Modeling in Conventional Reservoirs, *in* New Frontiers in Oil and Gas Exploration: Cham, Springer International Publishing, p. 137–163, doi:10.1007/978-3-319-40124-9_4.

Grana, D., and E. Della Rossa, 2010, Probabilistic petrophysical-properties estimation integrating statistical rock physics with seismic inversion: GEOPHYSICS, v. 75, no. 3, p. O21–O37, doi:10.1190/1.3386676.

Höecker, C., and G. Fehmers, 2002, Fast structural interpretation with structure-oriented filtering: The Leading Edge, **21**, no. 3, 238–243, doi: 10.1190/1.1463775.

Jesus, C. A. C., M. Olho Azul, W. M. Lupinacci, and L. Machado, 2017, Mapping of carbonate mounds in the Brazilian presalt zone. SEG Technical Program Expanded Abstracts 2017: 3298–3303, doi: 10.1190/segam2017-17789870.1.

Jesus, C. A. C, and P. Takayama, 2016, Reducing exploration risk with spectral decomposition, *in* Rio Oil & Gas 2016 Expo & Conference: p. 1.

John, A., L. W. Lake, C. Torres-Verdin, and S. Srinivasan, 2008, Seismic facies identification and classification using simple statistics: SPE Reservoir Evaluation & Engineering, **11**, no. 6, 984–990, doi: 10.2118/96577-PA.

Klein, P., L. Richard, and H. James, 2008, 3D curvature attributes: a new approach for seismic interpretation: First Break, **26**, no. 4, 105–111.

Kohonen, T., 2013, Essentials of the self-organizing map: Neural Networks, v. 37, p. 52–65, doi:10.1016/j.neunet.2012.09.018.

Kohonen, T., 1990, The self-organizing map: Proceedings of the IEEE, v. 78, no. 9, p. 1464–1480, doi:10.1109/5.58325.

Lupinacci, W. M., and S. A. M. Oliveira, 2015, Q factor estimation from the amplitude spectrum of the time–frequency transform of stacked reflection seismic data: Journal of Applied Geophysics, v. 114, p. 202–209, doi:10.1016/j.jappgeo.2015.01.019.

Lupinacci, W. M., A. P. Franco, S. A. M. Oliveira, and F. S. Moraes, 2017, A combined time-frequency filtering strategy for Q-factor compensation of poststack seismic data: Geophysics, **82**, no. 1, V1–V6, doi: 10.1190/geo2015-0470.1.

Marfurt, K. J., 2006, Robust estimates of reflector dip and azimuth: Geophysics, **71**, no. 4, P29–P40, doi: 10.1190/1.2213049.

Marfurt, K. J., and R. L. Kirlin, 2001, Narrow-band spectral analysis and thin-bed tuning: GEOPHYSICS, v. 66, no. 4, p. 1274–1283, doi:10.1190/1.1487075.

Marfurt, K. J., V. Sudhaker, A. Gersztenkorn, K. D. Crawford, and S. E. Nissen, 1999, Coherency calculations in the presence of structural dip: Geophysics, **64**, no. 1, 104 – 111, doi: 10.1190/1.1444508.

Matos, M. C., P. L. M. Osorio, and P. R. S. Johann, 2007, Unsupervised seismic facies analysis using wavelet transform and self-organizing maps: Geophysics, **72**, no. 1, P9–P21, doi: 10.1190/1.2392789.

Partyka, G., J. Gridley, and J. Lopez, 1999, Interpretational applications of spectral decomposition in reservoir characterization: The Leading Edge, v. 18, no. 3, p. 353–360, doi:10.1190/1.1438295.

Pendrel, J., H. Schouten, and R. Bornard, 2017, Bayesian estimation of petrophysical facies and their applications to reservoir characterization, *in* SEG Technical Program Expanded Abstracts 2017: Society of Exploration Geophysicists, p. 3082–3086, doi:10.1190/segam2017-17588007.1.

Puryear, C. I., and J. P. Castagna, 2008, Layer-thickness determination and stratigraphic interpretation using spectral inversion: Theory and application: GEOPHYSICS, v. 73, no. 2, p. R37–R48, doi:10.1190/1.2838274.

Qi, J., B. Zhang, H. Zhou, and K. J. Marfurt, 2014, Attribute expression of fault controlled – Karst Fort Worth Basin, Texas: A tutorial: Interpretation, **2**, no. 3, SF91–SF110, doi: 10.1190/INT-2013-0188.1.

Roden, R., T. Smith, and D. Sacrey, 2015, Geologic pattern recognition from seismic attributes: Principal component analysis and self-organizing maps: Interpretation, v. 3, no. 4, p. SAE59-SAE83, doi:10.1190/INT-2015-0037.1.

Roberts, A., 2001, Curvature attributes and their application to 3D interpreted horizons: First Break, **19**, no. 2, 85–100, doi: 10.1046/j.0263-5046.2001.00142.x.

Rongchang, L., B. Zhang, and X. Wang, 2017, Patterns classification in assisting seismic-facies analysis: SEG Technical Program Expanded Abstracts 2017, 2127-2131, doi: 10.1190/segam2017-17795000.1.

Saggaf, M. M., M. N. Toksöz, and M. I. Marhoon, 2003, Seismic facies classification and identification by competitive neural networks: GEOPHYSICS, v. 68, no. 6, p. 1984–1999, doi:10.1190/1.1635052.

Sancevero, S. S., A. Z. Remacre, and R. de S. Portugal, 2006, O papel da inversão para a impedância acústica no processo de caracterização sísmica de reservatórios: Revista Brasileira de Geofisica, v. 24, no. 4, p. 495–512, doi:10.1590/S0102-261X2006000400004.

Schwedersky, E. P., P. T. L. Menezes, and G. S. Neto, 2017, Poststack Seismic Inversion and Facies Prediction using Bayesian Inference, Boonsville Field, Fort Worth Basin, USA: A Case Study, *in* 15th International Congress of the Brazilian Geophysical Society & EXPOGEF, Rio de Janeiro, Brazil, 31 July-3 August 2017: Brazilian Geophysical Society, p. 1143–1146, doi:10.1190/sbgf2017-222.

Shanmuganathan, S., 2016, Artificial Neural Network Modelling: An Introduction, *in* S. Shanmuganathan, and S. Samarasinghe, eds., Artificial Neural Network Modelling: Cham, Springer, p. 1–14, doi:10.1007/978-3-319-28495-8_1.

Simm, R., and M. Bacon, 2014, Seismic Amplitude. an Interpreters Handbook: Cambridge University Press.

Sinha, S., P. S. Routh, P. D. Anno, and J. P. Castagna, 2005, Spectral decomposition of seismic data with continuous-wavelet transform: GEOPHYSICS, v. 70, no. 6, p. P19–P25, doi:10.1190/1.2127113.

Spikes, K., T. Mukerji, J. Dvorkin, and G. Mavko, 2007, Probabilistic seismic inversion based on rock-physics models: Geophysics, 72, no. 5, R87–R97, doi: 10.1190/1.2760162.

Sun, S., R. Siegfried, and J. Castagna, 2002, Examples of wavelet transform time-frequency analysis in direct hydrocarbon detection: SEG Technical Program Expanded Abstracts 2002, 457–460, doi: 10.1190/1.1817281.

Veeken, P. C. H., and M. Da Silva, 2004, Seismic Inversion Methods and some of their constraints: First Break, v. 22, no. 1013, p. 15–38, doi:10.3997/1365-2397.2004011.

Vernik, L., D. Fisher, and S. Bahret, 2002, Estimation of net-to-gross from P and S impedance in deepwater turbidites: The Leading Edge, 21, no. 4, 380–387,

http://dx.doi.org/10.1190/1.1471602

Wang, Y., 2007, Seismic time-frequency spectral decomposition by matching pursuit: Geophysics, **72**, no. 1, V13–V20, doi: 10.1190/1.2387109.

Wright, V. P., and A. J. Barnett, 2017, Critically evaluating the current depositional Models for the Pre-Salt Barra Velha Formation, Offshore Brazil: AAPG/SEG International Conference and Exhibition 2017.

Wright, P. and, K. Rodriguez, 2018, Reinterpreting the South Atlantic Pre-Salt 'Microbialite' reservoirs: petrographic, isotopic and seismic evidence for a shallow evaporitic lake depositional model. First Break, **36**, no. 5, 71–77.

Xu, R., and D. Wunsch, 2005, Survey of clustering algorithms: IEEE Transactions on Neural Networks, **16**, no. 3, 645–678, doi: 10.1109/TNN.2005.845141.

Xu, C., Q. Yang, and C. Torres-Verdín, 2016, Bayesian rock classification and petrophysical uncertainty characterization with fast well-log forward modeling in thin-bed reservoirs: Interpretation, v. 4, no. 2, p. SF19-SF29, doi:10.1190/INT-2015-0075.1.

Yuan, S., S. Wang, M. Ma, Y. Ji, L. Deng, 2017, Sparse Bayesian Learning-Based Time-Variant Deconvolution: IEEE Transactions on Geoscience and Remote Sensing, **55**, no. 11, 6182–6194, 10.1109/TGRS.2017.2722223.

Zhao, T., V. Jayaram, A. Roy, and K. J. Marfurt, 2015, A comparison of classification techniques of seismic facies recognition: Interpretation, **3**, no. 4, SAE29–SAE58, doi: 10.1190/INT-2015-0044.1.

Zheng, X., Y. Li, J. Li, X. Yu, 2007, Reef and shoal reservoir characterization using paleogeomorphology constrained seismic attribute analysis: SEG Technical Program Expanded Abstracts 2007: 1382–1386, doi: 10.1190/1.2792757.

Zhou, H., C. Wang, K. J. Marfurt, Y. Jiang, and J. Bi, 2014, Enhancing the resolution of seismic data using improved time-frequency spectral modeling, *in* SEG Technical Program Expanded Abstracts 2014: Society of Exploration Geophysicists, p. 2656–2661, doi:10.1190/segam2014-0353.1.